

Diagrammatics, Singularities, and Their Algebraic Interpretations *

J. Scott Carter

University of South Alabama

Mobile, AL 36688

carter@mathstat.usouthal.edu

Louis H. Kauffman

University of Illinois at Chicago

Chicago, Ill 60607-7045

kauffman@uic.edu

Masahico Saito

University of South Florida

Tampa, FL 33620

saito@math.usf.edu

October 25, 1996

Abstract

This series of lectures reviews the remarkable feature of quantum topology: There are unexpected direct relations among algebraic structures and the combinatorics of knots and manifolds. The $6j$ symbols, Hopf algebras, triangulations of 3-manifolds, Temperley-Lieb algebra, and braid groups are reviewed in the first three lectures. In the second lecture, we discuss parentheses structures and 2-categories of surfaces in 3-space in relation to the Temperley-Lieb algebras. In the fourth lecture, we give diagrammatics of 4 dimensional triangulations and their relations to the associahedron, a higher associativity condition. We prove that the 4-dimensional Pachner moves can be decomposed in terms of singular moves, and lower dimensional relations. In our last lecture, we give a combinatorial description of knotted surfaces in 4-space and their isotopies.

*MRCN: 57Q45

Key words: Reidemeister Moves, 2-categories, Movie Moves, Knotted Surfaces

1 Introduction

This paper is the written version of the mini-course given by the first named author at topx, São Carlos, 1996. In this series of talks, we discussed (1) how certain algebraic relationships can be depicted and computed via diagrams, (2) how diagrams lead to algebraic structures, (3) how singular diagrams yield algebraic relationships, and (4) how diagrams can be used to anticipate certain algebraic structures.

Our first talk concentrated on the theory of representations of $U(\mathfrak{sl}(2))$. The material presented here is a summary of that found in [12]. For a more diagrammatical approach one should consult [31]. All of the material that is presented in this talk carries over into the quantum case, and to see that analogy one should consult [12]. Our second talk was concerned with the Temperley-Lieb algebra and the diagrammatic depiction of the relations in the algebra. We apply this analysis to analyse surfaces that are embedded in 3-dimensional space. We show how embedded surfaces lead to a notion of a 2-category, and we describe the relations in that 2-category. Our third talk discussed the Pachner Theorem in dimension 2 and 3, and how this theorem can be used to relate algebraic structures to manifold invariants. In the fourth lecture, we interpreted the 4-dimensional Pachner Theorem via a variety of geometric and diagrammatic tricks. In the fifth lecture, we will present some new results on knotted surfaces and the theory of knotted surface isotopies that appear in [13].

1.1 Acknowledgements. The first named author is grateful for a Faculty Support and Development Grant from The University of South Alabama, grants from FAPESP for support while visiting ICMSC-USP and IME-USP, and a grant from the National Security Agency. The second named author is grateful for support from NSF grant DMS-2528707. The third named author is grateful for a Research and Creative Scholarship Grant (Grant Number 1249932R0) from the University of South Florida.

2 Representations of $U(\mathfrak{sl}(2, \mathbf{C}))$ and Their Diagrams

In this section we review the representations of $U(\mathfrak{sl}(2, \mathbf{C})) = U$ and their diagrammatics to start our discussion of deep relations between algebraic structures and diagrammatics. See [12] for more details.

2.1 The fundamental representations and its tensor powers. Suppose that $j \in \{0, 1/2, 1, 3/2, \dots\}$. Let V^j denote the $(2j + 1)$ -dimensional vector space over \mathbf{C} of linear homogeneous polynomials of degree $2j + 1$ in commuting variables x and y . Thus elements

of V^j are linear combinations of $x^r y^s$ where $r + s = 2j + 1$. In particular $V^{1/2}$ is the 2-dimensional vector space over \mathbf{C} of linear polynomials in commuting variables x and y .

Let $U = U(\mathfrak{sl}(2, \mathbf{C}))$ denote the algebra generated by E , F , and H subject to the relations $EF - FE = 2H$, $HE - EH = E$, $HF - FH = -F$. (This is called the universal enveloping algebra of $\mathfrak{sl}(2, \mathbf{C})$, the Lie algebra of 2×2 matrices over complex numbers with trace zero. Note that $E = \begin{pmatrix} 0 & 1 \\ 0 & 0 \end{pmatrix}$, $F = \begin{pmatrix} 0 & 0 \\ 1 & 0 \end{pmatrix}$, and $H = \begin{pmatrix} 1/2 & 0 \\ 0 & -1/2 \end{pmatrix}$ are the generators of $\mathfrak{sl}(2, \mathbf{C})$ and they satisfy the above relations.)

This algebra acts on V^j as differential operators:

$$E = x \frac{\partial}{\partial y},$$

$$F = y \frac{\partial}{\partial x},$$

and

$$H = \frac{1}{2} \left(x \frac{\partial}{\partial x} - y \frac{\partial}{\partial y} \right)$$

as one can check by computations.

In fact it is known that V^j , $j \in \{0, 1/2, 1, 3/2, \dots\}$, with these actions form the set of irreducible U -modules (called irreducible representations).

2.1.1 The projectors. Let us consider the tensor product $V^{1/2} \otimes V^{1/2}$ and the permutation map $X : V^{1/2} \otimes V^{1/2} \rightarrow V^{1/2} \otimes V^{1/2}$, $X(a \otimes b) = (b \otimes a)$. We define $\mathbf{+}_2$ by the formula

$$\mathbf{+}_2 = \frac{1}{2}(X + |\otimes|)$$

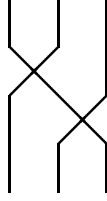
where $|$ denotes the identity mapping on $V^{1/2}$. The map $\mathbf{+}$ is an idempotent, and it commutes with the action of U . (When a map commutes with the action of U , it is said that the map is U -invariant.) The image consists of the symmetric expressions spanned by $x \otimes x$, $y \otimes y$, and $(x \otimes y + y \otimes x)$. This is a 3-dimensional vector space isomorphic (as a U -module) to V^1 . Roughly speaking, we took the averages of tensor products by permuting variables to identify tensor products with monomials.

More generally, let us consider the n fold tensor product of $V^{1/2}$,

$$W^n = \underbrace{V^{1/2} \otimes \dots \otimes V^{1/2}}_{n \text{ tensor factors}}.$$

Let X_k be the map defined by $X_k = |_{k-1} \otimes X \otimes |_{n-k-1}$ thus X_k acts as the identity on the first $k - 1$ and the last $n - k - 1$ tensor factors of W , and X_k permutes the k and the $(k + 1)$ st tensor factors.

A permutation $\sigma \in \Sigma_n$ acts on W^n as follows. Represent $\sigma \in \Sigma_n$ as a sequence of transpositions of adjacent letters; that is, σ is a product of permutations of the form $\sigma_k = (k, k+1)$; say $\sigma_{j_1} \sigma_{j_2} \cdots \sigma_{j_m}$. Then σ maps to the operator $X(\sigma) = X_{j_1} \circ X_{j_2} \circ \cdots \circ X_{j_m}$. The action of the permutation group commutes with the action of U and is said to be invariant under the U action. Moreover, the permutation action is expressed as a planar diagram as indicated in the following figure :



where the diagram represents the permutation $\sigma_1 \sigma_2$.

We generalize the idempotent $\mathbf{+}_2$ to act on W^n as follows:

$$\mathbf{+}_n = \frac{1}{n!} \sum_{\sigma \in \Sigma_n} X(\sigma)$$

The image of $\mathbf{+}_n$ consists of the symmetric expressions in x and y and can be identified with V^j via the map $\mu(x_1 \otimes \cdots \otimes x_n) = x_1 \cdot \cdots \cdot x_n$, where each x_k is either x or y .

Each term $X(\sigma)$ can be represented as a planar diagram of intersecting strings; the generic double points of those strings correspond to the transpositions of adjacent tensor factors.

2.2 Clebsch-Gordan theory. The tensor product of two irreducible representations can be decomposed as a direct sum of irreducible representations. Suppose that $a, b \in \{0, 1/2, 1, 3/2, \dots\}$. The triple of half integers (a, b, j) is said to be admissible if $j \in \{a + b, a + b - 1, \dots, |a - b| + 1, |a - b|\}$. This is a symmetric condition in a, b , and j .

Given an admissible triple (a, b, j) we define an U invariant map

$$\mathbb{Y}_j^{ab} : (V^{1/2})^{\otimes 2j} \rightarrow (V^{1/2})^{\otimes 2a} \otimes (V^{1/2})^{\otimes 2b}$$

as follows:

$$\mathbb{Y}_j^{ab} = (\mathbf{+}_{2a} \otimes \mathbf{+}_{2b}) \circ (|_{a+j-b} \otimes \overset{a+b-j}{\mathbb{U}} \otimes |_{b+j-a}) \circ \mathbf{+}_{2j}$$

where the map

$$\overset{n}{\mathbb{U}} : \mathbf{C} \rightarrow (V^{1/2})^{\otimes 2n}$$

is defined inductively as the composition

$$\begin{aligned} \mathring{U}^n: \mathbf{C} &\xrightarrow{\mathring{U}^{n-1}} \underbrace{V^{1/2} \otimes \dots \otimes V^{1/2}}_{2(n-1)} \xrightarrow{\mathring{U}} \\ &\underbrace{V^{1/2} \otimes \dots \otimes V^{1/2}}_{(n-1)} \otimes \mathbf{C} \otimes \underbrace{V^{1/2} \otimes \dots \otimes V^{1/2}}_{(n-1)} \\ &\xrightarrow{1 \otimes \mathring{U} \otimes 1} (V^{1/2})^{\otimes 2n}, \end{aligned}$$

$\mathring{U}^1 = \mathring{U}: \mathbf{C} \rightarrow V^{1/2} \otimes V^{1/2} \cup(1) = i(x \otimes y - y \otimes x)$, and $|_n$ represents the identity mapping on n -tensor factors of V .

The submodule in $(V^{1/2})^{\otimes 2j}$ spanned by the symmetric expressions in x and y is isomorphic to V^j . The image of this submodule under the map \mathring{Y} can be identified with the tensor product of V^a and V^b . For the Clebsh-Gordan coefficients defined by these maps and particular basis elements, see [12].

2.3 The $6j$ -symbols. The space of U invariant maps $V^k \rightarrow V^a \otimes V^b \otimes V^c$ can be constructed as follows. First, we have the composition

$$\begin{aligned} \begin{array}{c} a \quad b \quad c \\ \diagdown \quad \diagup \\ \quad \quad j \\ \diagup \quad \diagdown \\ k \end{array} &= (|_{2a} \otimes \mathring{Y}_j^{bc}) \circ \mathring{Y}_k^{aj} : \\ &(V^{1/2})^{\otimes 2k} \rightarrow (V^{1/2})^{\otimes 2a} \otimes (V^{1/2})^{\otimes 2b} \otimes (V^{1/2})^{\otimes 2c} \end{aligned}$$

for various values of j . Second, we have the composition

$$\begin{aligned} \begin{array}{c} a \quad b \quad c \\ \diagdown \quad \diagup \\ \quad \quad n \\ \diagup \quad \diagdown \\ k \end{array} &= (\mathring{Y}_n^{ab} \otimes |_{2c}) \circ \mathring{Y}_k^{nc}, \end{aligned}$$

for various values of n .

Restrict the values of j and n so that the triples (b, c, j) , (a, j, k) , (a, b, n) , and (n, c, k) are admissible. Alternatively, if one of these triples is not admissible, then declare the corresponding map \mathring{Y} to be the zero map.

The content of Lemma 2.6.1 of [12] is that, the sets

$$\left\{ \begin{array}{c} a \quad b \quad c \\ \diagdown \quad \diagup \\ \quad n \\ \quad | \\ \quad k \end{array} \right\} \quad \text{and} \quad \left\{ \begin{array}{c} a \quad b \quad c \\ \diagdown \quad \diagup \\ \quad j \\ \quad | \\ \quad k \end{array} \right\},$$

as the indices j and n range in such a way that (b, c, j) , (a, j, k) , (a, b, n) , and (n, c, k) form admissible triples, can be used to form bases for the vector space of U invariant linear maps $V^k \rightarrow V^a \otimes V^b \otimes V^c$, by composing these maps on the right with the inclusion of V^k into the tensor product and on the left with the tensor product of the multiplication maps.

The $6j$ symbol $\begin{Bmatrix} a & b & n \\ c & k & j \end{Bmatrix}$ is the change of basis matrix between these two bases. By convention, $\begin{Bmatrix} a & b & n \\ c & k & j \end{Bmatrix} = 0$ if any of the triples (b, c, j) , (a, j, k) , (a, b, n) , (n, c, k) is not admissible.

The $6j$ -symbol satisfies many beautiful identities that have a variety of geometric interpretations (see [4] for example.) Here we list the 2 most important identities for topological applications.

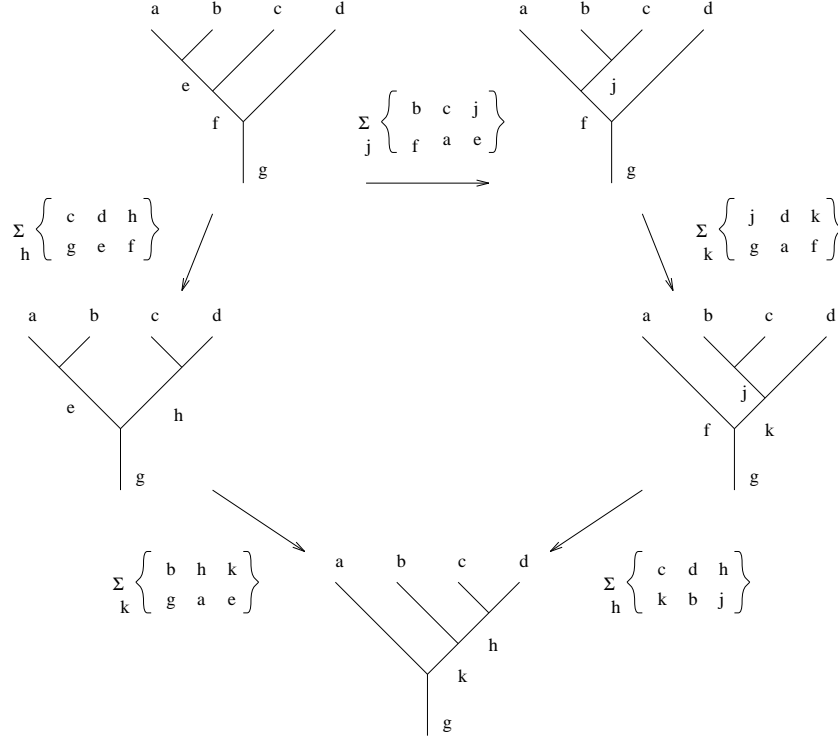
2.3.1 Theorem (Orthogonality). *Suppose that (a, b, n) , (c, k, n) , (a, b, m) , and (c, k, m) are admissible triples. Then then $6j$ -symbols satisfy the following relation:*

$$\sum_j \begin{Bmatrix} b & c & j \\ k & a & n \end{Bmatrix} \begin{Bmatrix} a & b & m \\ c & k & j \end{Bmatrix} = \delta_{m,n}.$$

2.3.2 Theorem (Biedenharn-Elliott Identity). *If (g, e, h) is an admissible triple, then the following relation holds among the $6j$ -symbols.*

$$\begin{Bmatrix} c & d & h \\ g & e & f \end{Bmatrix} \cdot \begin{Bmatrix} b & h & k \\ g & a & e \end{Bmatrix} \\ = \sum_j \begin{Bmatrix} b & c & j \\ f & a & e \end{Bmatrix} \cdot \begin{Bmatrix} j & d & k \\ g & a & f \end{Bmatrix} \cdot \begin{Bmatrix} c & d & h \\ k & b & j \end{Bmatrix}.$$

The proof of orthogonality can be carried out purely in terms of diagrams as in [12]. We will need to discuss the Biedenharn-Elliott identity in detail, and we reproduce the figure (2) from [12] that is used to prove this.



We include the figures from [12] that allow us to interpret orthogonality and the Biedenharn-Elliott identity in terms of the dual spines to triangulations. Let us explain. In the definition of the $6j$ -symbol, we used tree diagrams to represent maps involved. One of the trees is obtained from the other by moving the middle edge through a vertex. Consider this happening continuously; then such a continuous move of the middle edge sweeps out a 2-dimensional complex shown in Figure 1. This figure also shows that it is dual to a tetrahedron. Thus the $6j$ -symbol is assigned to a tetrahedron. Figs. 2 and 3 shows the complexes corresponding to the orthogonality and the Elliott-Biedenharn identity. The algebraic relations that are satisfied, then, correspond to moves on the dual spine of a triangulation. By passing to the quantum analogue of U at a root of unity invariants of 3-manifolds can be constructed because the moves the correspond to Biedenharn-Elliott and Orthogonality and one other move (that corresponds to an identity among quantum integers) suffice to construct a set of moves to triangulations.

To continue our discussion, we include the *binor identity* [43].

Define maps

$$\cap : V^{1/2} \otimes V^{1/2} \rightarrow \mathbf{C},$$

and

$$\cup : \mathbf{C} \rightarrow V^{1/2} \otimes V^{1/2}$$

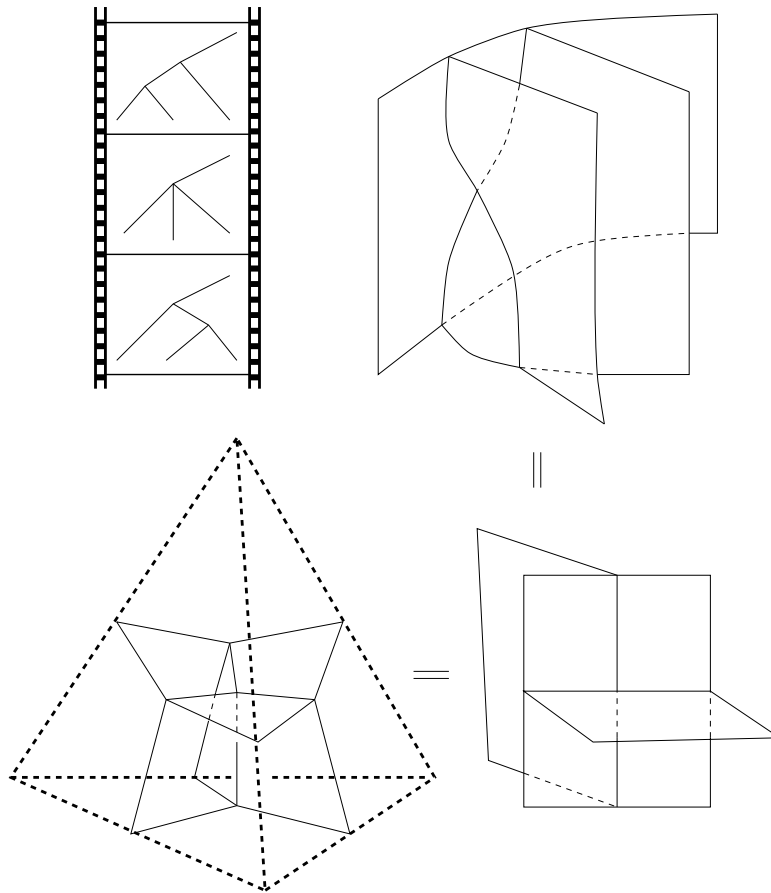


Figure 1: Tetrahedron and the $6j$ -symbol

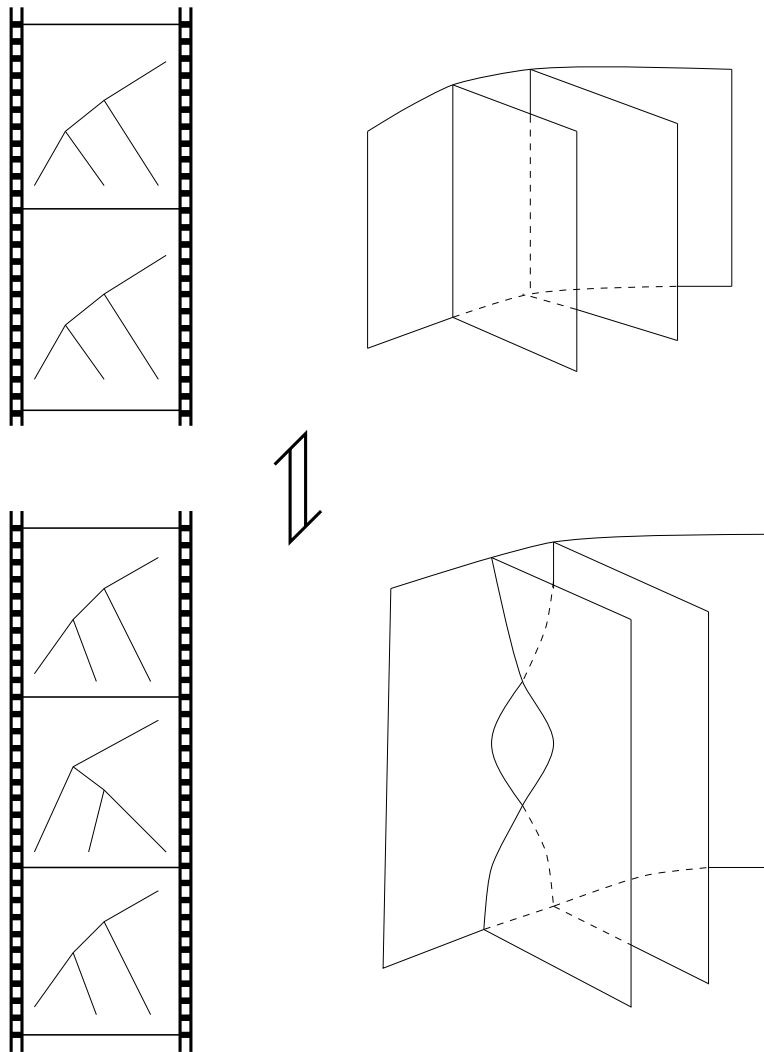


Figure 2: Orthogonality and dual complex

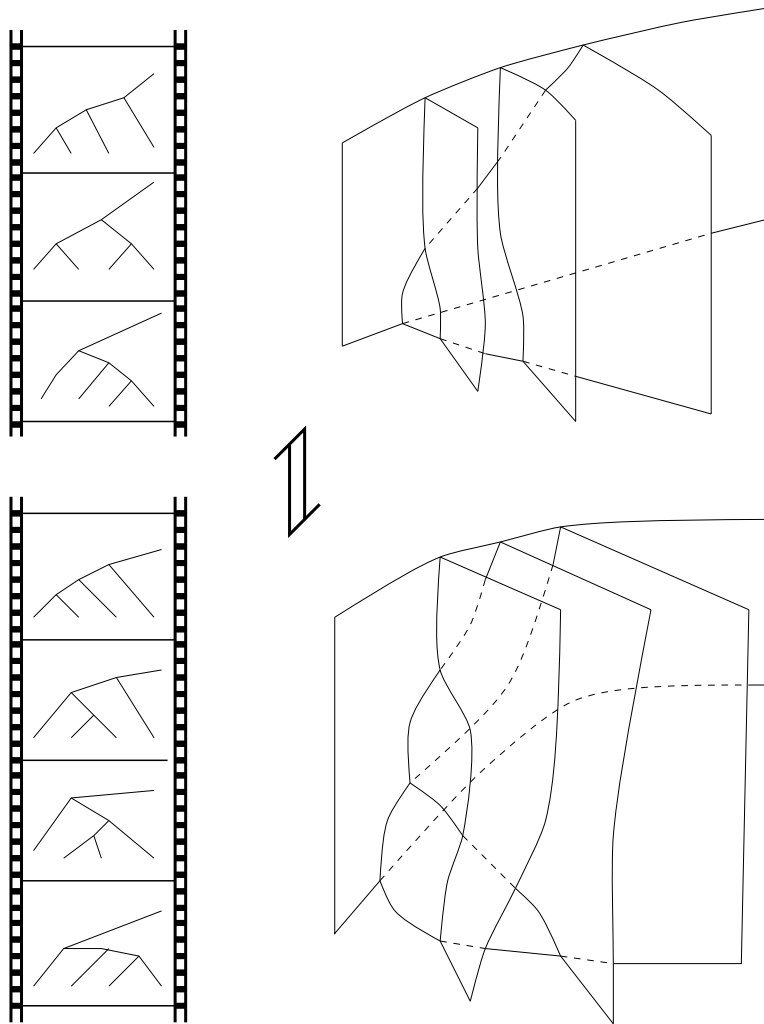


Figure 3: Biedenharn-Elliott and dual complex

by

$$\cup(1) = i(x \otimes y) - i(y \otimes x),$$

$$\cap(x \otimes x) = \cap(y \otimes y) = 0,$$

$$\cap(x \otimes y) = i = -\cap(y \otimes x).$$

It is a straight forward computation to show that

$$X = |\otimes| + \cup \circ \cap$$

where $|$ denotes the identity map on $V^{1/2}$.

The diagrammatic representation of this *binor identity* appears as follows:

$$\begin{array}{c} \diagdown \quad \diagup \\ \diagup \quad \diagdown \end{array} = \begin{array}{c} | \\ | \end{array} + \begin{array}{c} \cup \\ \cap \end{array}$$

Let us make some observations at this point.

First, the binor identity is an algebraic equation that relates a crossing to two ways of smoothing it. That the equation holds algebraically is a consequence of some very cleverly defined symbols. Its quantum analogue is the Kauffman bracket that can be used to give a diagrammatic or skein theoretic definition of the Jones polynomial. The efficacy of the binor identity and the bracket are deep mysteries. Why should such elementary formulas have such profound consequences?

The $6j$ -symbol is associated to a singular diagram in the context of 3-valent trees. The identities that it satisfies are also associated to some singular pictures, and one can make the same observations about the Clebsch-Gordan maps $\begin{array}{c} \diagdown \quad \diagup \\ | \end{array}$. The mystery that we want to penetrate is, “When are algebraic symbols associated to singularities, and when are the identities among these symbols associated to higher order singularities?”

2.4 How to Quantize. While we have sketched in these notes the use of the recoupling theory for $U(sl(2))$ and have indicated its extension to the quantum group $U_q(sl(2))$, it is actually possible to proceed to just q -deform the network structure associated with $U(sl(2))$ in a way that incorporates the knot theory. This method is very pleasing to the knot theorist and should (we believe) be of interest to the algebraist as well. This “ q -deformed spin network” viewpoint is explained in [30] and worked out in detail in [31]. In the latter reference the theory is detailed with regard to its behaviour at roots of unity (for q) and applied to construct the Turaev-Viro and the Witten-Reshetikhin-Turaev invariants of three-manifolds for $U(sl(2))$. A complement to these references is [12] where the recoupling theory

is done for $U_q(sl(2))$ in the algebraic context. It is very worthwhile to use all these references to get a global view.

At this writing, $U(sl(2))$ is the only group that has a fully combinatorial treatment for its recoupling theory. This combinatorial treatment can be expressed in many ways. The one we use originated in the theory of spin networks of Roger Penrose,[43]. Penrose devised his theory to give a specific model for a speculation that space-time could be the observed result of a background quantum process that was of a simple combinatorial nature. The Penrose spin nets did not construct space-time, but they did implicate certain geometrical properties of Euclidean space in the limit of large networks (with certain stability properties). This is an encouraging result. In these notes, we are continuing to work with the Penrose program in that we are looking at the relationship of generalized spin nets with both three and four manifold topology. We hope that the four manifold topology will eventually interface with issues of space, time, and quantum gravity.

2.4.1 q -spin nets. Here is a quick sketch of the construction of the q -deformed spin nets. First of all we take $A = q^{1/2}$ where A is the A of the bracket polynomial. This is just a convention to make our q match the usual qs used by everyone else. Then we replace the binor identity by the bracket identity:

$$\times = A \smile + A^{-1} \frown$$

which will be discussed further in section 3 Note that the bracket identity reduces to a binor identity when the value of A is 1 or -1 . Of course, for all other values of A the bracket identity is actually a definition of the action of a knot-theoretic crossing. This means that we are lifting the ostensibly flat theory of spin nets into a putative 3-space for the sake of knot theory. There are two ways to look at this move. One way is to simply say that we are taking over properties of spin nets for the sake of doing the topology of knots and links in ordinary three-space. If we say this, then we abandon the Penrose idea of the construction of space from the nets at the outset. However, we can *also* say that the extension to crossings is done in the spirit of the abstract category of knot and link diagrams. These diagrams are 4-regular plane graphs with extra structure at the vertices, and the plane is used to give these graphs a “coherent” cyclic ordering at each 4-valent vertex. In this sense the nets we are about to build are indeed an abstract structure and a purely combinatorial structure that encodes certain aspects of the topology of three-space but does not (strictly, logically) assume the prior existence of three dimensional space or three dimensional manifolds. How much of three dimensional topology and geometry can emerge from the nets?

In any case, the construction works as follows. We define the q -symmetrizer by the formula

$$\dagger_n^A = \frac{A^{n(n-1)}}{[n]!} \sum_{\sigma \in \mathfrak{S}_n} (A^{(-3)})^{T(\sigma)} \hat{\sigma}$$

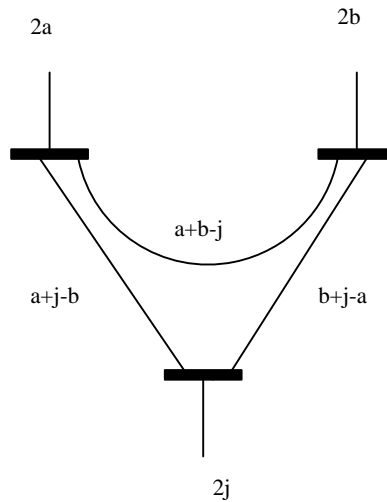
where

$$[n]! = \prod_{j=1}^n \frac{q^j - q^{-j}}{q - q^{-1}},$$

$\hat{\sigma}$ is the braid diagram obtained from the permutation diagram by lifting each crossings to a positive braid generator, and $T(\sigma)$ is the minimal number of transpositions of the form $(k, k + 1)$ that it takes to write the permutation σ .

This formula replaces the factorial by a q -deformed factorial, the sign by an algebra element raised to the least number of transpositions needed to return a given permutation to the identity, and it replaces the permutation by a (positive) braid that projects to the given permutation. Thus the q -symmetrizer is a sum over braids. Each braid can be expanded by the bracket identity into a sum of elements in the Temperley-Lieb algebra (defined below 3), and in this way the q -symmetrizer lives in the Temperley-Lieb algebra. It is easy to verify that if \dagger_n^A denotes the q -symmetrizer on n strands, then JW_n^A has square equal to itself and that $\dagger_n^A U = 0$ for U any non-identity generator of the Temperley Lieb algebra. This projector also satisfies a useful recursion formula of Hans Wenzel. We refer to the references cited above for this formula.

With the help of the q -symmetrizer, we define a 3-vertex by the interconnection formula shown below:



The collection of $a + b - j$ arcs that have a local minimum are q -deformed versions of the map \hat{U}_n , which we will define in detail in the next section. We are then prepared with a

purely combinatorial definition of the networks. Recoupling theory works in this context, and the higher order knot and link invariants obtained by taking q -symmetrized parallel strands can be worked out using this recoupling theory. The results are specific q -deformed spin network formulas for the Turaev and Witten-Reshetikhin-Turaev invariants of 3-manifolds. From the point of view of spin net philosophy this is quite significant. We have succeeded in showing that certain small nets (those coming from knots and links) capture subtle properties of specific three manifolds (those obtained by surgery on those links). A similar method produces the Crane-Yetter invariant of 4-manifolds [16]. The Crane-Yetter invariant of 4-manifolds obtains the signature of the 4-manifold in terms of a partition function that is constructed from q -deformed spin nets on the triangulation of the 4-manifold. One hopes for even deeper relations of spin networks with the topology of 4-manifolds.

3 The Temperley-Lieb Algebra and Associated Structures

3.1 Definition of Temperley-Lieb algebra. The *Temperley-Lieb algebra* $TL_n(\delta)$ is an algebra over \mathbf{C} multiplicatively generated by elements $1, h_1, h_2, \dots, h_{n-1}$ that are subject to the relations

$$h_j^2 = \delta h_j,$$

$$h_j h_{j-1} h_j = h_j,$$

for $j = 1, \dots, n-1$,

$$h_j h_{j+1} h_j = h_j,$$

for $j = 1, \dots, n-2$, and

$$h_j h_k = h_k h_j$$

if $|i - j| > 1$, where δ is a parameter that we set equal to $-A^2 - A^{-2}$, and A is a complex number which we discuss later. In Section 3.5, we will show that the dimension of $TL_n(\delta)$ as a vector space over \mathbf{C} is $\binom{2n}{n}/(n+1)$ by giving a correspondence between the products of generators and legitimate parentheses structures.

As a preliminary step to this, we point out that there is a correspondence between the basis elements in the algebra and certain diagrams. In particular 1 corresponds to the diagram of n vertical strings, and h_j corresponds to the diagram

$$\underbrace{\left| \begin{array}{c} | \\ \dots \\ | \end{array} \right|}_{j-1} \cup \underbrace{\left| \begin{array}{c} | \\ \dots \\ | \end{array} \right|}_{n-j-1}$$

for $1 \leq j \leq n - 1$. The composition $h_j h_k$ is represented by juxtaposing the diagram representing h_j above the diagram representing h_k . Then it is easy and fun to observe that the relations in the algebra are represented by topologically equivalent diagrams. The parameter value δ is the value that is assigned to a closed loop.

3.2 Temperley-Lieb algebras and braid groups. As before, let $V^{1/2}$ denote the vector space of linear polynomials in variables x and y . We can let the diagrams representing the basis elements of the algebra act on the n -fold tensor power of $V^{1/2}$, but now we assign the matrix values $\begin{pmatrix} 0 & iA \\ -iA & 0 \end{pmatrix}$ to \cup and \cap where $i^2 = -1$. Combining results of [12] and [25] one finds that the representation of the Temperley-Lieb algebra as an algebra of automorphisms on $(V^{1/2})^{\otimes n}$ is faithful for all values of A . (When $A = \pm 1$ we are discussing representations of U as in the preceding section.)

The bracket identity

$$\sigma_j \mapsto Ah_j + A^{-1} | \otimes |$$

provides a representation of the n -string braid group into the Temperley-Lieb algebra from which the Jones polynomial can be constructed. Here the n -string braid group is generated by σ_j , ($j = 1, \dots, n - 1$) and is subject to the relations $\sigma_j \sigma_{j+1} \sigma_j = \sigma_{j+1} \sigma_j \sigma_{j+1}$, ($j = 1, \dots, n - 1$), and $\sigma_j \sigma_k = \sigma_k \sigma_j$ if $|j - k| > 1$. The braid group elements are represented by arcs monotonically going down between parallel horizontal planes. See [30] for more details.

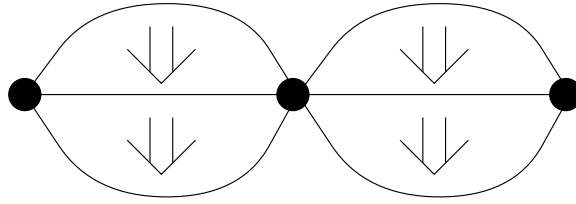
Analogues of the projections $\mathbf{+}_n$ that were constructed in the preceding section can be used to construct Clebsch-Gordan maps and $6j$ -coefficients that satisfy the Biedenharn-Elliot Identity and Orthogonality. When the parameter A is set to be a $4r$ th root of unity, these can be used to define invariants of 3-manifolds — we will sketch the definition in Section 4.

3.3 An associated 2-category. The definition of a monoidal 2-category occupies 3 pages in [33]; so we will not reproduce it here. Instead we will give an example (based on the diagrams that represent the basis elements of the Temperley-Lieb Algebra) of a monoidal 2-category and we will describe the relations in that 2-category. The uninitiated have little to fear, not only are 2-categories rather natural classes to study, the 2-category that we present here is a familiar one.

So let us summarize what is meant by a (small) 2-category. This consists of three sets: Objects, (1-)morphisms from objects to objects, and 2-morphisms from 1-morphisms to 1-morphisms. Explicitly, given any two objects A, B , there is a set of 1-morphisms $\text{hom}(A, B)$ between them; the object A is called the source object, B is the target. Given any two

1-morphisms $f_0, f_1 \in \text{hom}(A, B)$ there is a set of 2-morphism between them; f_0 is the *source arrow*, and f_1 is the *target arrow*. The object A is the *source object* and the object B is the *target object*.

The objects in the category are schematized as points, the morphism as arrows, and the 2-morphism as cells whose boundaries are the arrows. There are two ways to compose 2-morphisms: If the the source arrow (resp. object) of a 2-morphism coincides with the target arrow (resp. object) of another, then the 2-morphisms can be composed by joining target to source. Both compositions should be strictly associative, and the pair of compositions satisfies a relation that ensures that the diagram:



is unambiguous. (The relation is called the 4-square relation.)

In our setting the objects correspond to non-negative integers. The 1-morphisms are symbols $\cap_{j,k}$ (resp. $\cup_{j,k}$) from the object (corresponding to) $(j+k+2)$ to $(j+k)$ (resp. from $(j+k)$ to $(j+k+2)$). Diagrammatic interpretations of these morphisms are as follows. The symbol $\cap_{j,k}$ (resp. $\cup_{j,k}$) represent the tangle diagram from $(j+k+2)$ points to $(j+k)$ points (resp. from $(j+k)$ points to $(j+k+2)$ points) consisting of a single maximal point (resp. minimal point) with j arcs to the left of the critical point and k arcs to the right of the critical point. These left and right arcs have no critical points. Any 1-morphism from m to n can be written as a composition of these basic 1-morphisms. (If $m+n$ is an odd number, then $\text{hom}(m, n)$ is the empty set.) Thus any 1-morphism can be identified with a word in the letters $\cup_{j,k}, \cap_{j,k}$.

Here is a list of the generating 2-morphisms in the present 2-category. Immediately below a geometric interpretation is given!

1.

$$B : ((j+k) \xrightarrow{I_{j+k}} (j+k))$$

$$\implies$$

$$((j+k) \xrightarrow{\cup_{j,k}} (j+k+2) \xrightarrow{\cap_{j,k}} (j+k))$$

2.

$$D : ((j+k) \xrightarrow{\cup_{j,k}} (j+k+2) \xrightarrow{\cap_{j,k}} (j+k))$$

$$\begin{aligned} & \implies \\ & ((j+k) \xrightarrow{I_{j+k}} (j+k)) \end{aligned}$$

3.

$$\begin{aligned} HB : & ((j+k+2) \xrightarrow{I_{j+k+2}} (j+k+2)) \\ & \implies \\ & ((j+k+2) \xrightarrow{\cap_{j,k}} (j+k) \xrightarrow{\cup_{j,k}} (j+k+2)) \end{aligned}$$

4.

$$\begin{aligned} HD : & ((j+k+2) \xrightarrow{\cap_{j,k}} (j+k) \xrightarrow{\cup_{j,k}} (j+k+2)) \\ & \implies \\ & ((j+k+2) \xrightarrow{I_{j+k+2}} (j+k+2)) \end{aligned}$$

5.

$$\begin{aligned} A(+) : & ((j+k+1) \xrightarrow{\cup_{j+1,k}} (j+k+3) \xrightarrow{\cap_{j,k+1}} (j+k+1)) \\ & \implies \\ & ((j+k+1) \xrightarrow{I_{j+k+1}} (j+k+1)) \end{aligned}$$

6.

$$\begin{aligned} A(-) : & ((j+k+1) \xrightarrow{\cup_{j,k+1}} (j+k+3) \xrightarrow{\cap_{j+1,k}} (j+k+1)) \\ & \implies \\ & ((j+k+1) \xrightarrow{I_{j+k+1}} (j+k+1)) \end{aligned}$$

7.

$$\begin{aligned} V(+) : & ((j+k+1) \xrightarrow{I_{j+k+1}} (j+k+1)) \\ & \implies \\ & ((j+k+1) \xrightarrow{\cup_{j+1,k}} (j+k+3) \xrightarrow{\cap_{j,k+1}} (j+k+1)) \end{aligned}$$

8.

$$\begin{aligned} V(-) : & ((j+k+1) \xrightarrow{I_{j+k+1}} (j+k+1)) \\ & \implies \\ & ((j+k+1) \xrightarrow{\cup_{j,k+1}} (j+k+3) \xrightarrow{\cap_{j+1,k}} (j+k+1)) \end{aligned}$$

9.

$$\begin{aligned}
X(\cap)(+) &: ((j+k+\ell+4) \overset{\cap_{j+\ell+2,k}}{\rightarrow} (j+k+\ell+2) \overset{\cap_{j,k+\ell}}{\rightarrow} (j+k+\ell)) \\
&\implies \\
&((j+k+\ell+4) \overset{\cap_{j,k+\ell+2}}{\rightarrow} (j+k+\ell+2) \overset{\cap_{j+\ell,k}}{\rightarrow} (j+k+\ell))
\end{aligned}$$

10.

$$\begin{aligned}
X(\cap)(-) &: ((j+k+\ell+4) \overset{\cap_{j,k+\ell+2}}{\rightarrow} (j+k+\ell+2) \overset{\cap_{j+\ell,k}}{\rightarrow} (j+k+\ell)) \\
&\implies \\
&((j+k+\ell+4) \overset{\cap_{j+\ell+2,k}}{\rightarrow} (j+k+\ell+2) \overset{\cap_{j,k+\ell}}{\rightarrow} (j+k+\ell))
\end{aligned}$$

11.

$$\begin{aligned}
X(\cup)(+) &: ((j+k+\ell) \overset{\cup_{j,k+\ell}}{\rightarrow} (j+k+\ell+2) \overset{\cup_{j+\ell+2,k}}{\rightarrow} (j+k+\ell+4)) \\
&\implies \\
&((j+k+\ell) \overset{\cup_{j+\ell,k}}{\rightarrow} (j+k+\ell+2) \overset{\cup_{j,k+\ell+2}}{\rightarrow} (j+k+\ell+4))
\end{aligned}$$

12.

$$\begin{aligned}
X(\cup)(-) &: ((j+k+\ell) \overset{\cup_{j+\ell,k}}{\rightarrow} (j+k+\ell+2) \overset{\cup_{j,k+\ell+2}}{\rightarrow} (j+k+\ell+4)) \\
&\implies \\
&((j+k+\ell) \overset{\cup_{j,k+\ell}}{\rightarrow} (j+k+\ell+2) \overset{\cup_{j+\ell+2,k}}{\rightarrow} (j+k+\ell+4))
\end{aligned}$$

13.

$$\begin{aligned}
X(\cap\cup)(+) &: ((j+k+\ell+2) \overset{\cup_{j+\ell+2,k}}{\rightarrow} (j+k+\ell+4) \overset{\cap_{j,k+\ell+2}}{\rightarrow} (j+k+\ell+4)) \\
&\implies \\
&((j+k+\ell+2) \overset{\cap_{j,k+\ell}}{\rightarrow} (j+k+\ell) \overset{\cup_{j+\ell,k}}{\rightarrow} (j+k+\ell+2))
\end{aligned}$$

14.

$$\begin{aligned}
X(\cap\cup)(-) &: ((j+k+\ell+2) \overset{\cap_{j,k+\ell}}{\rightarrow} (j+k+\ell) \overset{\cup_{j+\ell,k}}{\rightarrow} (j+k+\ell+2)) \\
&\implies \\
&((j+k+\ell+2) \overset{\cup_{j+\ell+2,k}}{\rightarrow} (j+k+\ell+4) \overset{\cap_{j,k+\ell+2}}{\rightarrow} (j+k+\ell+4))
\end{aligned}$$

15.

$$\begin{aligned}
X(\cup\cap)(+) &: ((j+k+\ell+2) \overset{\cup_{j,k+\ell+2}}{\rightarrow} (j+k+\ell+4) \overset{\cap_{j+\ell+2,k}}{\rightarrow} (j+k+\ell+2)) \\
&\implies \\
&((j+k+\ell+2) \overset{\cap_{j+\ell,k}}{\rightarrow} (j+k+\ell) \overset{\cup_{j,k+\ell}}{\rightarrow} (j+k+\ell+2))
\end{aligned}$$

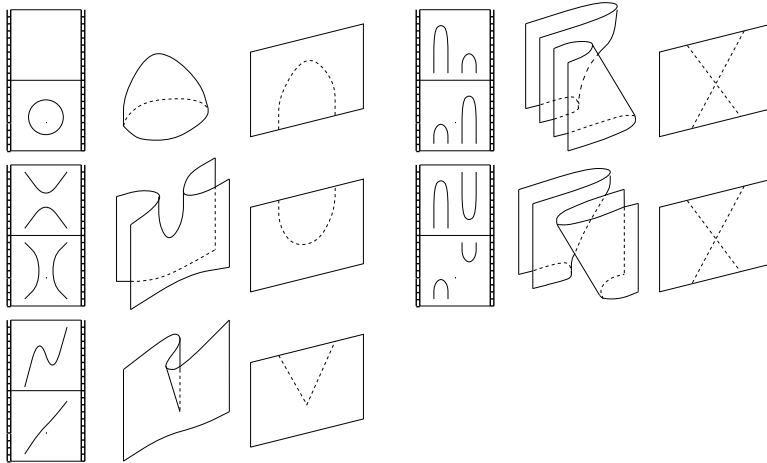


Figure 4: Generating 2-morphisms

16.

$$\begin{aligned}
 X(\cup)(-) : ((j+k+\ell+2) \xrightarrow{\cap_{j+\ell,k}} (j+k+\ell) \xrightarrow{\cup_{j,k+\ell}} (j+k+\ell+2)) \\
 \implies \\
 ((j+k+\ell+2) \xrightarrow{\cup_{j,k+\ell+2}} (j+k+\ell+4) \xrightarrow{\cap_{j+\ell+2,k}} (j+k+\ell+2))
 \end{aligned}$$

Examine the figures depicted in Fig. 4. These represent maximal/minimal points of surfaces, saddle points of surfaces, cusps, and the exchanges in the heights of critical points. These critical phenomena represent the 2-morphisms in the 2-category that were listed above. The 2-morphisms denoted by V represent the birth of a pair of max/min points via a cusp. The source 1-morphism appears at the bottom of a diagram and the target 1-morphism appears at the top. The 2-morphisms represented by A represent the death of such a pair. The 2-morphisms HB and HD are saddle points. The 2-morphisms B and D are the birth and death of a simple closed curve respectively. The various 2-morphisms denoted by X are the interchange of the heights of critical points in the planar diagrams.

A planar diagram of simple closed curves corresponds to a sequence of 1-morphisms in our 2-category. The source and target of this sequence is the object 0. For example, a circle is represented by the arrows

$$0 \xrightarrow{\cup_{0,0}} 2 \xrightarrow{\cap_{0,0}} 0$$

If we write that composition in $g(f(x))$ notation, it will read

$$\cap_{0,0}(\cup_{0,0}(0)).$$

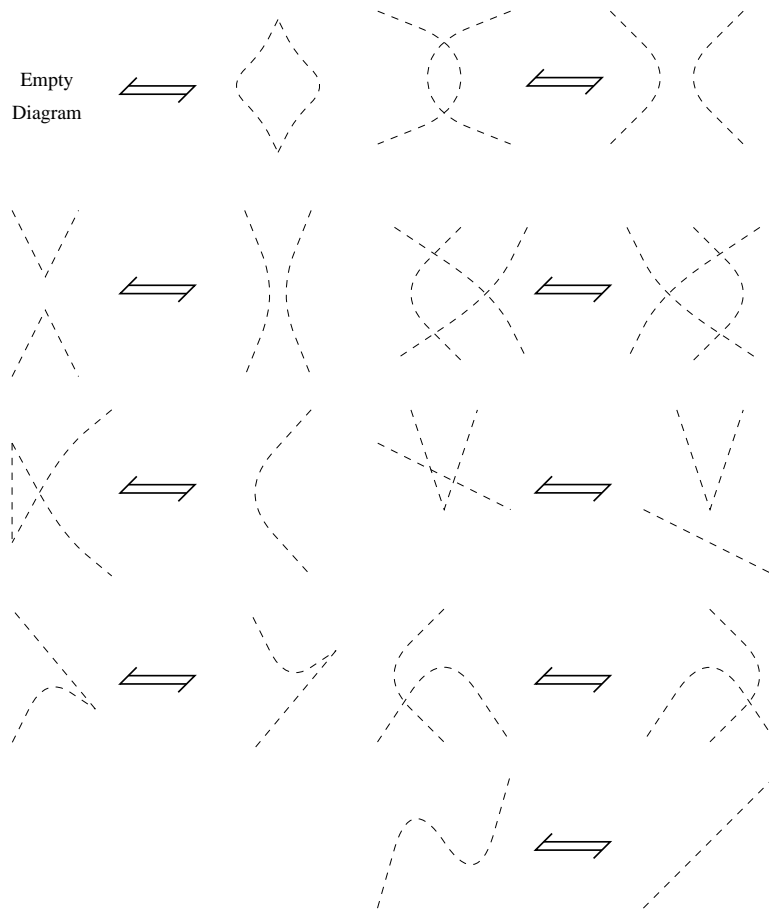


Figure 5: Codimension 1 singularities

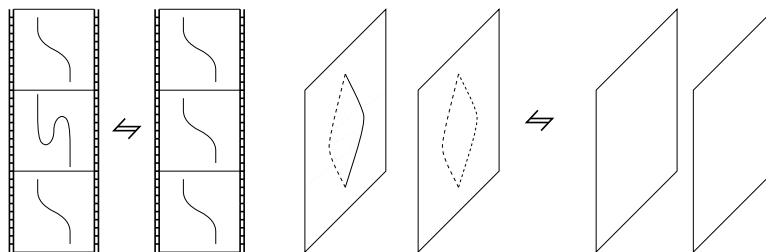


Figure 6: Elliptic confluence of cusps

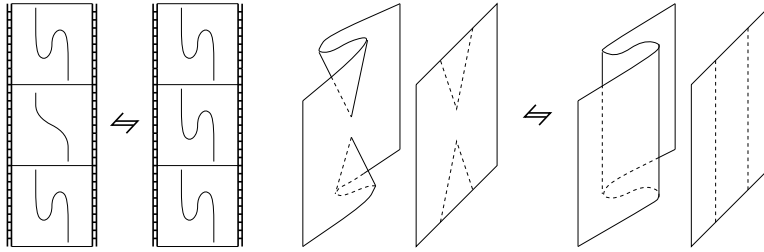


Figure 7: Hyperbolic confluence of cusps

And that composition is what we see when we read the diagram from top to bottom.

The 2-category constructed represents surfaces embedded in 3-space as follows. Given a surface embedded in 3-dimensional space, project it to a plane and choose a height function (called the vertical axis) in that plane. Then the projection of the surface in the plane generically has cusp and fold singularities. The critical points of the fold set with respect to the height function are the birth (B), death (D), saddle (HB and HD), and cusp (V and A) singularities. The crossing points of the fold set correspond to the 2-morphisms denoted by X .

The preimage of any non-critical value on the vertical axis in 3-space is a collection of embedded closed curves in space. By choosing a direction on the horizontal axis (perpendicular to the vertical axis in the plane of projection), this collection of closed curves defines a 1-morphism from 0 to 0 in the 2-category. The sequence of critical points in the vertical direction defines a 2-morphism from the trivial 1-morphism to the trivial 1-morphism.

Now suppose that we are interested in surfaces embedded in 3-space up to a relationship of ambient isotopy. Then we can define a collection of relations among the 2-morphism that generate this topological equivalence. In fact, these relations are catalogued in Mancini and Ruas [38] as the set of codimension 1 singularities of planar projections of embedded surfaces. We can include a height function to the plane into which the surface is projected and further classify those singularities when the height function is fixed. The list of codimension 1 singularities of planar projections of surfaces is compiled in Fig 5.

In order to interpret these singularities as relations among 2-morphisms, we represent generating 2-morphisms as commutative diagrams. Then relations among 2-morphisms are represented by 3-dimensional polytopes. In Figs. 9 and 8, we illustrate two of these polytope. Fig. 6 and Fig. 7 illustrate two of the chart moves found in Fig. 5.

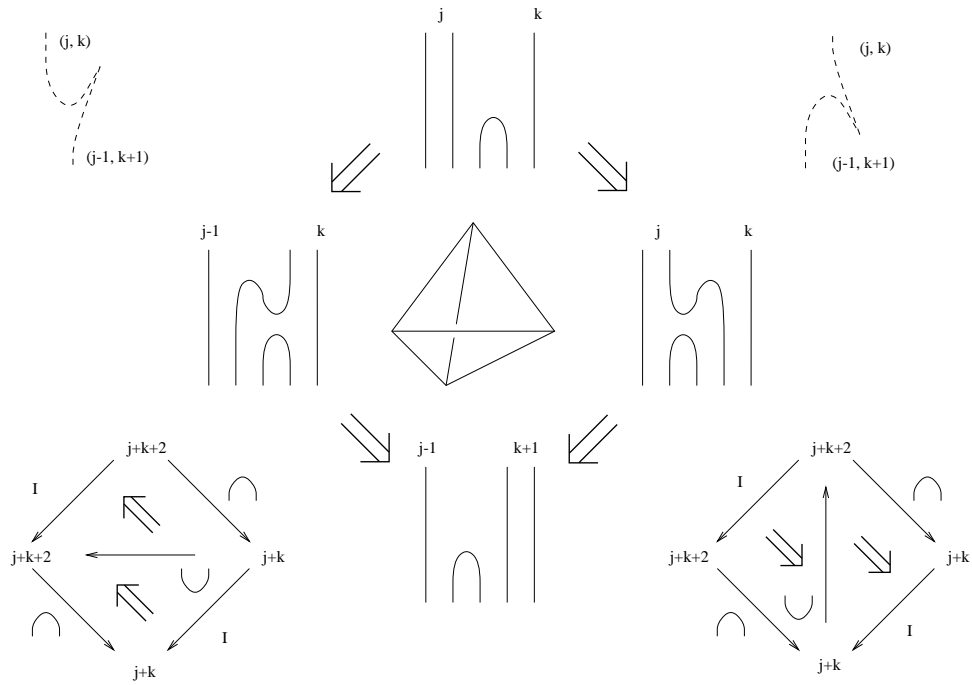


Figure 8: The polytope for one of the moves

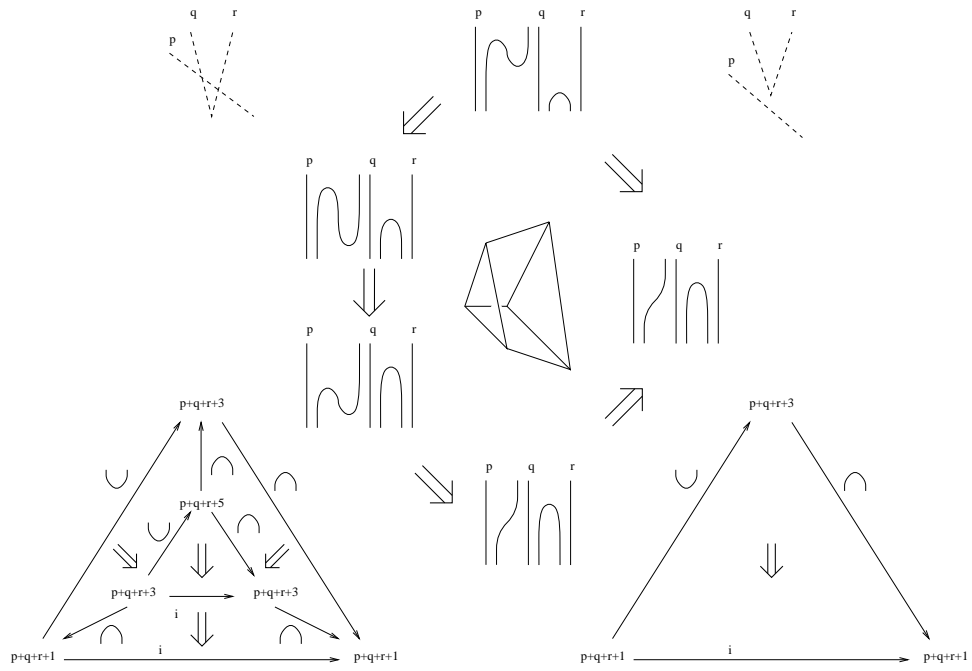


Figure 9: The polytope for another move

Now we can turn the 2-category into a purely combinatorial description of isotopy classes of embedded surfaces in 3-space. Specifically, we define a *sentence* to be a sequence of words in the letters $\cup_{i,j}$ and $\cap_{m,n}$ where the sequence starts and ends in the empty word and is subject to the following restrictions. Each word in the sentence starts with $\cap_{0,0}$ and ends in $\cup_{0,0}$. Each letter in a word represents a 1-morphism and if a and b are adjacent letters in a word (so $W = UabV$), then the target of A coincides with the source of B . The sequence of words differ at most by the following:

1. Cancellation or creation of a pair of adjacent symbols $\cap_{m,n}\cup_{m,n}$ in the word.
2. Cancellation or creation of a pair of adjacent symbols $\cup_{m,n}\cap_{m,n}$ in the word, for appropriate values on m, n .
3. Cancellation or creation of a pair $\cap_{m,n}\cup_{m+1,n-1}$ or $\cap_{m+1,n-1}\cup_{m,n}$.
4. A replacement of $\cap_{i,j}\cup_{m,n}$ by $\cup_{m,n-2}\cap_{i-2,j}$ if $i \geq m+2$ and $n+m = i+j$, or vice-versa.
5. A replacement of $\cap_{i,j}\cup_{m,n}$ by $\cup_{m-2,n}\cap_{i,j-2}$ if $i \leq m+2$ and $n+m = i+j$, or vice-versa.
6. A replacement of $\cup_{i,j}\cup_{m,n}$ by $\cup_{m,n+2}\cup_{i-2,j}$ if $i \geq m+2$ and $m+n = i+j$, or vice-versa.
7. A replacement of $\cap_{m-2,n}\cap_{i,j}$ by $\cap_{i,j-2}\cap_{m,n}$ if $i \leq m$, $n+2 \leq j$, and $m+n = i+j$, or vice-versa.

3.4 Sentence Equivalence. We define two sentences to be equivalent if we can get from one to the other by a sequence of the following moves.

1. $(WV, W \cap_{m,n} \cup_{m-1,n+1} V, WV) \leftrightarrow (WV)$.
2. $(W \cap_{m,n} \cup_{m-1,n+1} V, WV, W \cap_{m,n} \cup_{m-1,n+1} V) \leftrightarrow (W \cap_{m,n} \cup_{m-1,n+1} V)$.
3. $(W \cap_{m,n} V, W \cap_{m,n} \cap_{m+2,n} \cup_{m+1,n+1} V, W \cap_{m,n} \cap_{m,n+2} \cup_{m+1,n+1} V, W \cap_{m,n} V) \leftrightarrow (W \cap_{m,n} V)$.
4. $(WY_{i,j}Y'_{m,n}V, WY'_{m',n'}Y_{i',j'}V, WY_{i,j}Y'_{m,n}V) \leftrightarrow (WY_{i,j}Y'_{m,n}V)$

where $|i-m| > 1$, $|i'-m'| > 1$ and $i+j = n+m$.

Here Y and Y' denotes either \cap or \cup . The relations between subscripts of Y and Y' are not very strictly specified in the above relation, and it is because they depend

on the cases of \cap and \cup . See the generating 2-morphisms, Items (9) through (16), in Section 3.3 for the different subscript possibilities among \cap s and \cup s. This fact is pointed out to us by L. Langford. Since the list becomes 4 times as lengthy, we give one specific example of subscripts :

$$(W \cap_{i,j} \cap_{m,n} V, W \cap_{m-2,n} \cap_{i,j+2} V, W \cap_{i,j} \cap_{m,n} V) \leftrightarrow (W \cap_{i,j} \cap_{m,n} V)$$

where $i \leq m - 2$ and $i + j = m + n$.

The same remark applies in the rest of this list. The symbols Y, Y', Y'', Z, \bar{Z} represent \cap or \cup and subscripts are left unspecified in some cases.

$$\begin{aligned} 5. & (WY_{i,j}Y'_{k,\ell}Y''_{m,n}V, WY'_{k,\ell}Y_{i,j}Y''_{m,n}V, \\ & WY'_{k,\ell}Y''_{m,n}Y_{i,j}V, WY''_{m,n}Y'_{k,\ell}Y_{i,j}V) \\ & \leftrightarrow (WY_{i,j}Y'_{k,\ell}Y''_{m,n}V, WY_{i,j}Y''_{m,n}Y'_{k,\ell}V, \\ & WY''_{m,n}Y_{i,j}Y'_{k,\ell}V, WY''_{m,n}Y'_{k,\ell}Y_{i,j}V) \end{aligned}$$

where $|i - k| > 1, |i - m| > 1, |k - m| > 1$, and $i + j = k + \ell = n + m$.

$$\begin{aligned} 6. & (WY_{i,j} \cap_{m+1,n-1} \cup_{m+2,n-2} V, W \cap_{m+1,n-1} Y_{i,j} \cup_{m+2,n-2} V, W \cap_{m+1,n-1} \cup_{m+2,n-2} Y_{i,j} V, WY_{i,j} V) \\ & \leftrightarrow (WY_{i,j} \cap_{m+1,n-1} \cup_{m+2,n-2} V, WY_{i,j} V) \end{aligned}$$

where $|i - m| > 1$ and $i + j + 2 = m + n$.

$$\begin{aligned} 7. & (WY_{i,j} V, WY_{i,j} Z_{m,n} \bar{Z}_{m,n} V, W Z_{m,n} Y_{i,j} \bar{Z}_{m,n} V) \\ & \leftrightarrow (WY_{i,j} V, W Z_{m,n} \bar{Z}_{m,n} Y_{i,j} V, W Z_{m,n} Y_{i,j} \bar{Z}_{m,n} V) \end{aligned}$$

where (Z, \bar{Z}) is either of (\cap, \cup) , or (\cup, \cap) , $|i - m| > 1$ and $i + j = m + n$.

$$8. (W Z_{m,n} V, W Z_{m,n} \bar{Z}_{m,n} Z_{m,n} V, W Z_{m,n} V) \leftrightarrow (W Z_{m,n} V)$$

where the pair (\bar{Z}, Z) was introduced and the pair (Z, \bar{Z}) was cancelled in the left hand side, and (Z, \bar{Z}) is either of (\cap, \cup) , or (\cup, \cap) .

$$\begin{aligned} 9. & (W \cap_{m+1,n} V, W \cap_{m+1,n} \cup_{m,n+1} \cap_{m,n+1} V, W \cap_{m,n+1} V) \\ & \leftrightarrow (W \cap_{m+1,n} V, W \cap_{m,n+1} \cup_{m+1,n} \cap_{m+1,n} V, W \cap_{m,n+1} V). \end{aligned}$$

$$10. (W Z_1 Z_2 V, W Z'_1 Z_2 V, W Z'_1 Z'_2 V) \leftrightarrow (W Z_1 Z_2 V, W Z_1 Z'_2 V, W Z'_1 Z'_2 V) \text{ where the changes } Z_i \text{ to } Z'_i \text{ for } i = 1, 2 \text{ are any of our elementary moves.}$$

There are several variations to these moves that correspond to (a) changing the direction of the height function in the plane, (b) changing the direction of projection onto the plane, and (c) and changing the direction of the horizontal axis in the plane of projection. We leave the reader to explicitly write down the corresponding moves to sentences.

The relation between the above sentence equivalences and the chart moves 5 is as follows. As before we fix a height function on the plane of charts, and cut along horizontal lines. When we read off the intersection of a horizontal line and the dotted curves of the chart from left to right, we get a sequence of words in \cap s and \cup s. When we do this from the top horizontal line to the bottom one, we get a sequence of words (a sentence). Then the LHS and the RHS of each chart move gives each of the above equivalences between sentences.

Higher categories including the one defined above were defined and studied by Baez and Dolan [2]. Here we included explicit relations among 2-morphisms.

3.4.1 Remark. In this setting we see that singularities naturally give rise to a 2-category where the 1-morphisms, 2-morphisms, and relations among the 2-morphisms correspond to singularities of plane curves, surfaces, and the projections of surfaces in a plane respectively.

3.5 Catalan numbers. The dimension of the Temperley-Lieb Algebra TL_n is the Catalan number $\binom{2n}{n}/(n+1)$. One way to prove this is to notice that each product of generators corresponds to a legitimate string of parentheses. The correspondence is given as follows. Consider a product of generators as a planar diagram in \cup s and \cap s. Join the two horizontal arcs together by a point at infinity on the right. Then bend this line down to a horizontal line in the plane to get collection of arcs above the line joined to the line. Comb the arcs until each has exactly one critical point, this diagram represents the associated parentheses string. For example we have in TL_3 the basis $\{1, h_1, h_2, h_1h_2, h_2h_1\}$. These elements correspond respectively to the collection of parentheses strings $((()))$, $()()()$, $((()))$, $(())()$, and $()(())$. The correspondence between the collection of nested and juxtaposed \cap s and parentheses is given by joining the top edges of a matched pair of parenthesis together. Thus the first string above corresponds to three nested \cap s, the second string corresponds to $\cap \cap \cap$; the third string corresponds to a pair of \cap s nested under a third, and so forth.

It is not difficult to count the number of legitimate parentheses strings. One way is to associate a string with a path from $(0, 0)$ to $(2n, 0)$ that stays above the x -axis, and that consists of segments of length $\sqrt{2}$ that are of slope ± 1 . An upward sloping segment corresponds to left parenthesis; a downward sloping segment to a right parenthesis. The total number of paths from $(0, 0)$ to $(2n, 0)$ (including those that dip below the x -axis) is

$\binom{2n}{n}$. The number of paths that do not correspond to legitimate parentheses is $\binom{2n}{n+1}$ (One can count these paths by finding the first time an illegal path touches the line $y = -1$, then reflecting the initial segment of the path through that line. This gives a path from $(0, -2)$ to $(2n, 0)$; the number of these is $\binom{2n}{n+1}$ because it takes 2 steps up to get to the x -axis.) The difference in these numbers is $\binom{2n}{n}/(n+1)$.

The n th Catalan number occurs as the count of a number of different objects. Three of those are important to the present discussion. The first is the number of legitimate parentheses strings that we have just counted. The second is the number of different ways of triangulating an $(n+2)$ -gon with no vertices internal to the faces or edges of the polygon. The third is the number of ways of composing $n+1$ symbols with a binary composition (Thus when $n=3$, we have $(ab)(cd)$, $((ab)c)d$, $(a(bc))d$, $a((bc)d)$, and $a(b(cd))$.) Naturally, the binary composites correspond to three valent trees, and by dualizing the trees we obtain triangulations of polygons. A correspondence between the set of naked parentheses and the set of binary composites is exemplified as follows.

$$()() \leftrightarrow a < b > < c > < d > \leftrightarrow ((ab)c)d$$

$$()(()) \leftrightarrow a < b > < c < d > > \leftrightarrow (ab)(cd)$$

$$((())) \leftrightarrow a < b < c < d > > > \leftrightarrow a(b(cd))$$

$$(()()) \leftrightarrow a < b < c > < d > > \leftrightarrow a((bc)d)$$

$$(())(()) \leftrightarrow a < b < c > > < d > \leftrightarrow (a(bc))d$$

The correspondence between the naked parentheses and the expressions in $\langle \rangle$ is given by inserting a letters into the parenthetical expressions. The second correspondence is given by thinking of a letter in brackets (*e.g.* $\langle d \rangle$) as an operator acting on the right by multiplication. Thus in the top line we read that b acts on a , and this product is acted upon by c ; the resulting product is acted upon by d .

3.5.1 Operations to parentheses. There are various products and operators that can be defined on a string of parentheses. A full account of these can be found in [32]. Here we mention a few of these operations:

First, strings of parentheses A and B can be juxataposd to form the string AB .

Second, given strings A and B , we can write $A = A'$) and $B = (B'$ for some strings B' and A' that each have a single unmatched parenthesis. The product $[A, B] \rightarrow A'B'$ gives a legitimate parentheses string. The unmatched left (of A' gets paired to the unmatched right) in B' .

Third, if a string can be decomposed as a product AB we can map that product to the product BA . Now strictly speaking this is not an operation, but a method of obtaining one parenthesis string from another.

Another method of obtaining one string from another is the operation of handle sliding. Given a string AB where A and B are legitimate parentheses, we may assume that $A = A'$) where A' has an unmatched (, and $B = (B')B''$ where B' and B'' are legitimate. (the strings B' and B'' may be empty. We map $AB = A')(B')B''$ to $A'(B')B''$. A given string may have several descendants from this process. Let us examine the easy cases:

$$()() \mapsto (()),$$

$$()()() \mapsto (())(),$$

$$()()() \mapsto ()(()),$$

$$()()() \mapsto (())(),$$

$$()()() \mapsto ((())),$$

and

$$()()() \mapsto ((())).$$

The total number of descendants and antecedents on a string of parentheses consisting of n matched pairs is $n - 1$. The arrows \mapsto can be used to arrange the set of parentheses to be the vertices on a polytope called the *associatahedron* or *Stasheff polytope*. The edges of the polytope are arrows \mapsto such as those found above. The faces of the polytope are pentagons and quadrilaterals. The higher dimensional cells can be defined inductively. We will give examples of the Stasheff polytopes in Sections 4 and 5.

The operations on parentheses strings have other topological interpretations. We can consider the cap form of a parentheses string as a planar surface. If there are n matched pairs of parentheses, then the surface is a disk with n handles and $n + 1$ boundary components. The handles correspond to the matched pairs of parentheses, and so a given parentheses string represents a choice of ordered basis for $H_1(F)$ where F is the planar surface.

The operation $[A, B] = [A'], (B') \rightarrow A'B'$ corresponds to removing a 1-handle, by connecting 2-boundary components. The operation $AB = A')(B')B'' \mapsto A'(B''))B''$ corresponds to handle sliding, or on H_1 this represents a change of basis by an elementary operation. The operation $AB \rightarrow BA$ represents reordering the basis by a cyclic permutation.

3.5.2 Remark. One can consider a set of abstract words in some alphabet where the words are constructed according to some grammatical rules. Then sentences can be constructed as a sequence of transformation rules on the words. A set of relations among the transformation rules allow us to define an equivalence relation on sentences. When the abstract words represent some topological phenomenon, the rules of grammar and the transformation rules often are generated by certain types of singularities. The goal of such investigations, then, is to find other natural algebraic objects that obey the same grammar and transformations.

4 The Pachner Theorem

The Pachner Theorem gives a set of moves to triangulations of n -dimensional manifolds such that two triangulations of a given manifold are related by a sequence of moves taken from the Pachner list. One can use the Pachner Theorem in low dimensions to construct invariants of manifolds that are related to algebraic structures. Here we describe in detail the Pachner Theorem in dimension 2 and 3 and outline the construction of invariants and the related algebraic structures. In Section 5, we describe the situation in dimension 4 in detail.

Perhaps an easy way to understand the Pachner Theorem is to climb the dimension ladder one wrung at a time. To this end we begin by discussing moves to triangulations of surfaces.

4.1 The 2 dimensional moves. Let a closed surface F be given with triangulations T_1 and T_2 . Then T_2 may be obtained from T_1 from the local moves to triangulations illustrated in Fig. 10. Here is a description of these moves. Two triangles glued along an edge form a quadrilateral with the common edge forming the diagonal; they can be replaced by the two triangles formed by the boundary of that quadrilateral and the opposite diagonal. A given triangle can be barycentrally subdivided, or three triangles any two of which share an edge containing a vertex common to all three can be replaced by a single triangle. We call these moves the $(2 \rightleftharpoons 2)$ -move and the $(1 \rightleftharpoons 3)$ -move respectively.

The moves can be given in purely combinatorically terms as follows:

$$(2 \rightleftharpoons 2) : (012) \cup (023) \rightleftharpoons (013) \cup (123)$$

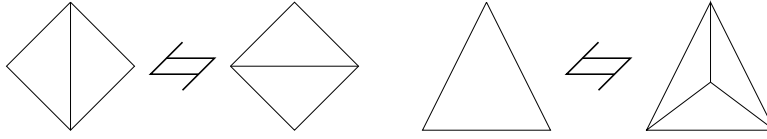


Figure 10: 2-Dimensional Pachner moves

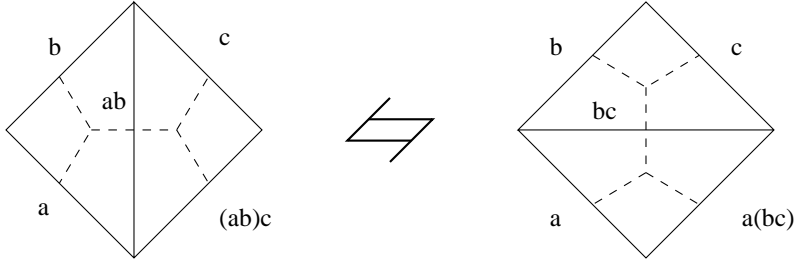


Figure 11: Associativity and the $(2 \rightleftharpoons 2)$ -move

$$(1 \rightleftharpoons 3) : (123) \rightleftharpoons (012) \cup (013) \cup (023)$$

where each integer represents a label on a vertex, and the triples themselves represent triangles with those vertices.

Thus the 2D Pachner moves relate the faces of a tetrahedron. Specifically, the $(2 \rightleftharpoons 2)$ -move consists of two pairs of triangles and they together form a tetrahedron (Figure 15). Meanwhile, the $(1 \rightleftharpoons 3)$ -move relates three triangular faces of a tetrahedron to the remaining face. The three triangles form the central projection of a tetrahedron.

In Fig. 11, we have indicated the relation between the $(2 \rightleftharpoons 2)$ -move and the associativity axiom in an algebra. We turn now to give algebraic axioms that allow us to construct invariants of surfaces.

4.1.1 Semi-simple algebras and surfaces. Let A denote a finite dimensional associative algebra over the complex numbers \mathbf{C} . Let $\{\phi_i | i = 1, \dots, n\}$ denote an ordered basis for A , and for $x, y, z \in \{1, \dots, n\}$, let C_{xy}^z denote *the structural constant* of the algebra A . Thus the multiplication between basis elements is given by the formula:

$$\phi_x \cdot \phi_y = \sum_z C_{xy}^z \phi_z.$$

Apply the associativity law, $(ab)c = a(bc)$, to the basis elements as follows:

$$(\phi_a \phi_b) \phi_c = \left(\sum_j C_{ab}^j \phi_j \right) \phi_c = \sum_{j,d} C_{ab}^j C_{jc}^d \phi_d$$

$$\phi_a(\phi_b\phi_c) = \phi_a\left(\sum_i C_{bc}^i \phi_i\right) = \sum_{i,d} C_{ai}^d C_{bc}^i \phi_d.$$

In this way, we obtain the equation

$$\sum_j C_{ab}^j C_{jc}^d = \sum_i C_{ai}^d C_{bc}^i$$

whose geometrical interpretation will be presented shortly.

For $x, y \in \{1, 2, \dots, n(= \dim A)\}$, define

$$g_{xy} = \sum_{u,v} C_{ux}^v C_{vy}^u.$$

Then this is invertible precisely when the algebra A is semi-simple, and the matrix inverse g^{xy} of g_{xy} defines a bilinear form on the algebra A . The geometric interpretation of this bilinear form and that of the associativity identity will allow us to define from a semi-simple associative algebra, an invariant of 2-dimensional manifolds.

We follow the definition in [21]. Let T be a triangulation of a closed $2D$ manifold F . Let $\mathcal{N} = \{1, 2, \dots, n\}$. This is called the set of *spins*. Let $\mathcal{ET} = \{(e, f) | e \in f\}$ be the set of all the pairs of an edge and a face of T such that e is an edge of f . A *labeling* is a map $L : \mathcal{ET} \rightarrow \mathcal{N}$. Thus a labeling is an assignment of spins to all the edges with respect to faces. Given a labeling, we assign weightings to faces and edges as follows: Suppose that we are given functions C and g ; $C : \mathcal{N}^3 \rightarrow \mathbf{C}$, $C(x, y, z) = C_{xyz}$, and $g : \mathcal{N}^2 \rightarrow \mathbf{C}$, $g(x, y) = g^{xy}$. If a face has three edges labeled with spins x, y, z , then assign the complex number C_{xyz} to the face. The function C possesses a cyclic symmetry; so $C_{xyz} = C_{yzx} = C_{zxy}$. If an edge is shared by two faces, and the edge with respect to these faces receives spins x and y , then assign the complex number g^{xy} to the edge. Then define a *partition function* $\Psi(T)$ by $\sum_L \prod C_{xyz} g^{uv}$ where the sum is taken over all the labelings and the product is taken over all the faces and edges.

In order for the partition function to be topologically invariant, it cannot depend on the choice of triangulation. So we interpret associativity and the bilinear form in a semi-simple algebra over \mathbf{C} in terms of the Pachner moves. Specifically, the $(2 \rightleftharpoons 2)$ -Pachner moves is related to the associativity law $(ab)c = a(bc)$. The relationship is depicted in Figure 11. The dual graphs, indicated in the Figure by dotted segments, are sometimes useful for visualizing the relations between triangulations and the algebraic structure. The diagram given in Figure 12 illustrates the geometrical interpretation of the bilinear form $g_{xy} = \sum_{u,v} C_{xu}^v C_{yv}^u$. Finally, this relationship together with the associativity identity can be used to show that the partition function is invariant under the $(1 \rightleftharpoons 3)$ -Pachner move. The essence of the proof is indicated in Figure 13.

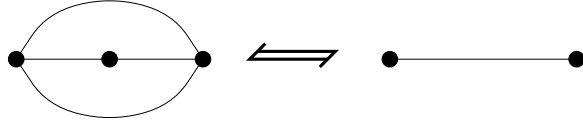


Figure 12: The semi-simplicity axiom and degenerate triangulations

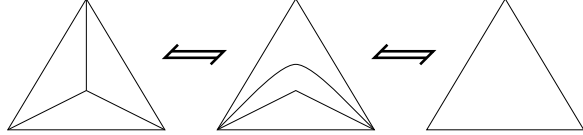


Figure 13: Semi-simplicity, associativity and the $(1 \rightleftharpoons 3)$ -move

Having illustrated the the algebra axioms diagrammatically we turn to show how the structure constants and the bilinear form of associative semi-simple algebras solve the equations corresponding to the Pachner moves. Given, structural constants C_{xy}^z and a non-degenerate bilinear form g^{uz} with inverse g_{uz} , define C_{xyu} by the equation,

$$C_{xyu} \equiv g_{uz} C_{xy}^z.$$

Then since

$$\sum_j C_{ab}^j C_{jc}^d = \sum_i C_{ai}^d C_{bc}^i$$

the partition function defined in this way is invariant under the $(2 \rightleftharpoons 2)$ -move. Furthermore, we have

$$C_{de}^a C_{ab}^j C_{jc}^d = C_{de}^a C_{ai}^d C_{bc}^i = g_{ie} C_{bc}^i = C_{ebc},$$

and so the partition function is invariant under the $(1 \rightleftharpoons 3)$ -move. In this way, a semi-simple finite dimensional algebra defines an invariant of surfaces. On the other hand, given a partition function one can define a semi-simple algebra with these structure constants and that bilinear form. In [21], this is stated as Theorem 3:

The set of all LTFTs is in one-to-one correspondence with the set of finite dimensional semi-simple associative algebras.

Here LTFT stands for a Lattice Topological Field Theory which is an invariant of manifolds satisfying certain axioms involving glueing and boundaries.

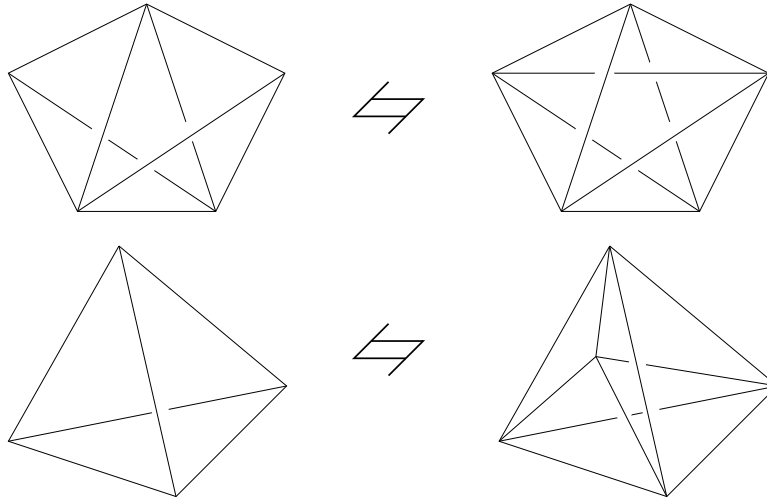


Figure 14: Pachner moves

Observe that the $(1 \rightleftharpoons 3)$ -move follows from the $(2 \rightleftharpoons 2)$ -move and certain singular move for triangulations corresponding to a non-degeneracy condition. In the sequel, we will see similar phenomena in dimension 3 and 4.

In general, the idea of defining a partition function to produce a manifold invariant is (1) to assign spins to simplices of a triangulation, and (2) to find weightings that satisfy equations corresponding to Pachner moves. This approach, of course, depends on finding such solutions to (often extremely overdetermined) equations. Such solutions come from certain algebraic structures. Thus one hopes to extract appropriate algebraic structures from the Pachner moves in each dimension. This is the motivating philosophy of quantum topology.

4.2 Dimension 3. In this section we review the Pachner moves [42] of triangulations of manifolds in dimension 3. In Figure 14 the Pachner moves are depicted, these are called the $(2 \rightleftharpoons 3)$ -move and the $(1 \rightleftharpoons 4)$ -move.

The 3-dimensional Pachner moves are related to the 4-simplex in the same way as the 2-dimensional moves are related to the tetrahedron. One side of each 3-dimensional move is a union of the 3-dimensional faces of the boundary of a 4-simplex, the other side of the move is the rest of the 3-dimensional faces, and they together form the boundary of a 4-simplex. For example, the $(1 \rightleftharpoons 4)$ indicates two 3-balls on the boundary of a 4-simplex as they appear in a central projection of the simplex.

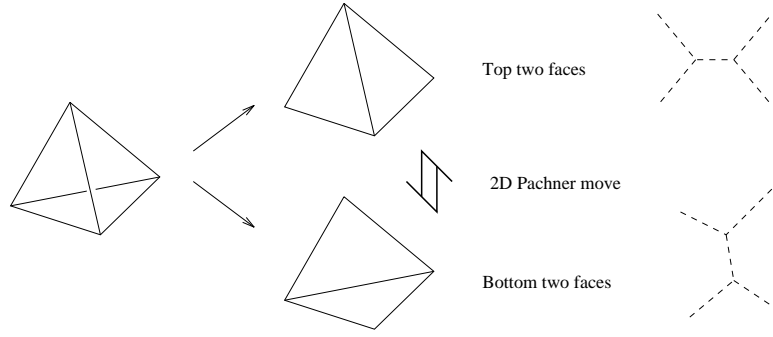


Figure 15: Movie of a tetrahedron and a 2D Pachner move

4.2.1 Hopf algebras and 3-manifolds. In this section we review invariants defined by Chung-Fukuma-Sharpere [14] and Kuperberg [36] (we follow the description in [14]). We note that the invariants obtained in this section are also very closely related to the invariants defined and studied by Hennings, Kauffman, Radford and Otsuki (see [35] for example).

4.2.2 Definition (Bialgebras). A *bialgebra* over a field k is a quintuple $(A, m, \eta, \Delta, \epsilon)$ such that

1. (A, m, η) is an algebra where $m : A \otimes A \rightarrow A$ is the multiplication and $\eta : k \rightarrow A$ is the unit. (*i.e.*, these are k -linear maps such that $m(1 \otimes m) = m(m \otimes 1)$, $m(1 \otimes \eta) = 1 = m(\eta \otimes 1)$).
2. $\Delta : A \rightarrow A \otimes A$ is an algebra homomorphism (called the *comultiplication*) satisfying $(id \otimes \Delta)\Delta = (\Delta \otimes id)\Delta$,
3. $\epsilon : A \rightarrow k$ is an algebra homomorphism called the *counit*, satisfying $(\epsilon \otimes id)\Delta = id = (id \otimes \epsilon)\Delta$.

4.2.3 Definition (Hopf algebras). An *antipode* is a map $s : A \rightarrow A$ such that $m \circ (s \otimes 1) \circ \Delta = \eta \circ \epsilon = m \circ (1 \otimes s) \circ \Delta$.

A *Hopf algebra* is a bialgebra with an antipode.

The image of the comultiplication is often written as $\Delta(a) = a_1 \otimes a_2$ for $a \in A$. The image in fact is a linear combination of such tensors but the coefficients and the summation are abbreviated; this is the so-called Sweedler notation [1].

The condition that the comultiplication be an algebra homomorphism is also called the compatibility condition between multiplication and comultiplication. This condition is written by $\Delta(ab) = \Delta(a)\Delta(b)$. More specifically, $\Delta \circ m = (m \otimes m) \circ P_{23} \circ (\Delta \otimes \Delta)$ where P_{23}

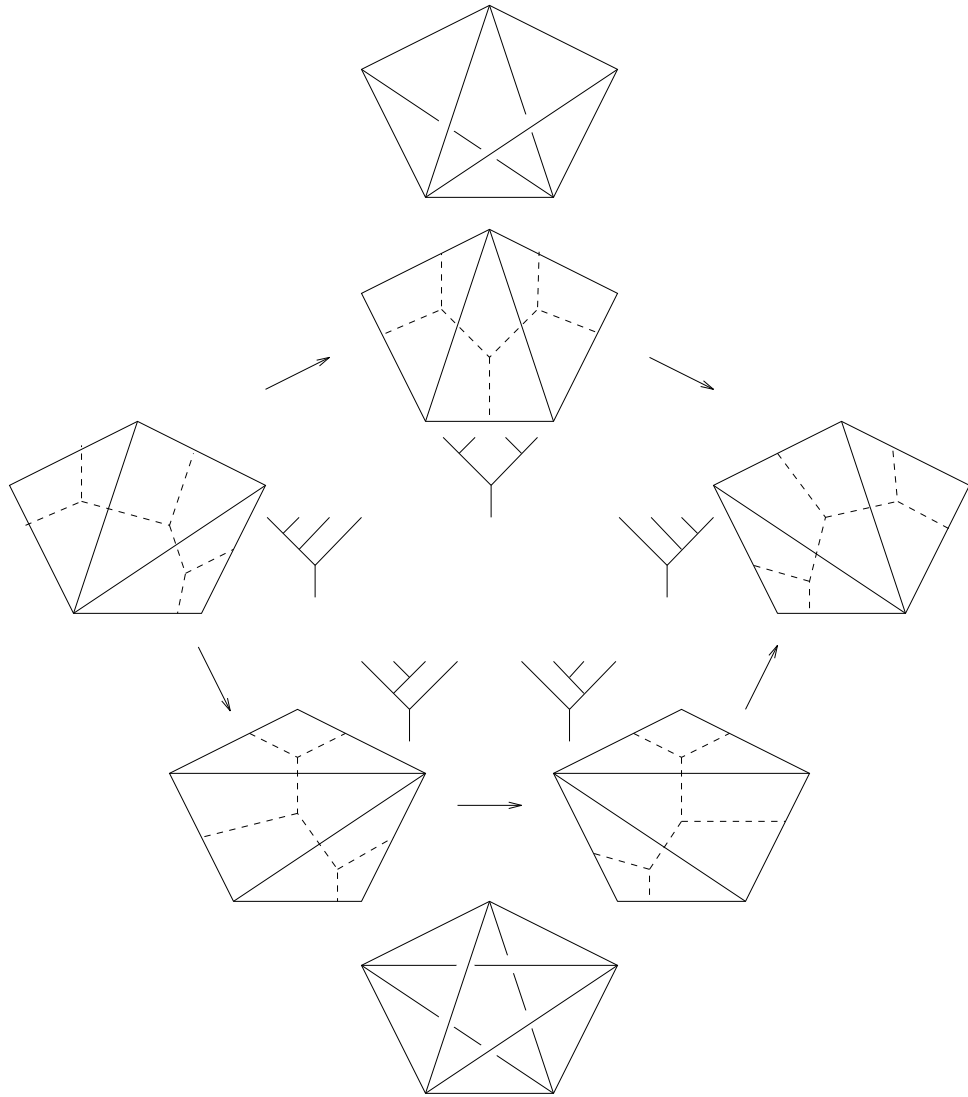


Figure 16: The pentagon, trees, and a Pachner move

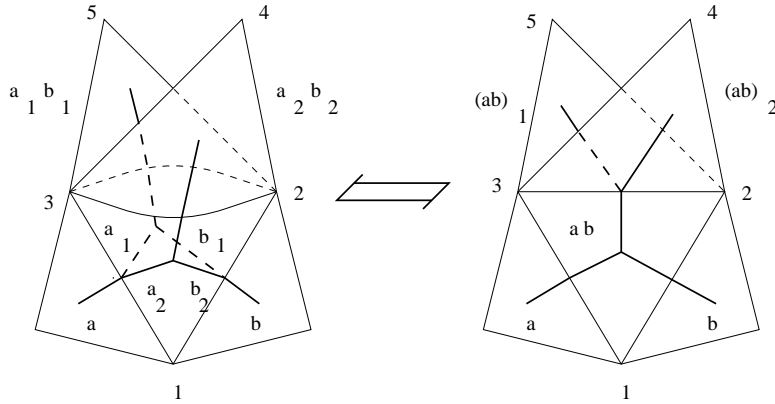


Figure 17: The cone move in dimension 3

denotes the permutation of the second and the third factor: $P_{23}(x \otimes y \otimes z \otimes w) = (x \otimes z \otimes y \otimes w)$. In the Sweedler notation, it is also written as $(ab)_1 \otimes (ab)_2 = a_1 b_1 \otimes a_2 b_2$.

4.2.4 Invariants. The definition of invariants defined in [14] is similar to the 2-dimensional case. Given a triangulation T of a 3-manifold M , give spins to edges with respect to faces (triangles). The weights then are assigned to edges in addition to faces. The structural constants C_{xyz} (resp. Δ_{xyz}) of multiplication (resp. comultiplication) are assigned as weights to faces (resp. edges). If an edge is shared by more than three faces, then a composition of comultiplications are used. For example for four faces sharing an edge, use the structural constant for $(\Delta \otimes 1)\Delta$. The coassociativity ensures that the other choice $(1 \otimes \Delta)\Delta$ gives the same constant $\Delta_{v_1, v_2, v_3, v_4}$. Thus the partition function takes the form $\Psi(T) = \sum_L \prod C_{xyz} \Delta_{v_1, \dots, v_n}$.

In [14] the well defined-ness was proved by using singular triangulations — these generalize triangulations by allowing certain cells as building blocks. In this case the move called the *cone move* for singular triangulation plays an essential role. This move is depicted in Figure 17 with a dual graph to illustrate the relationship to the compatibility condition.

Let us now explain the relation of this move to the compatibility condition verbally. In the left hand side of Fig. 17 there are parallel triangular faces sharing the edge (12) and (13); these triangles have different edges connecting the vertices 2 and 3. One of these is shared by the face (234) while the other is shared by the face (235).

The parallel faces (123) and (123)' are collapsed to a single face to obtain the right hand side of Fig. 17. Now there is a single face with edges (12), (23), and (31), and the edge (23) is shared by three faces (123), (234), and (235).

The thick segments indicate part of the dual graph. Each segment is labeled by Hopf algebra elements. Reading from bottom to top, one sees that the graphs represent maps from $A \otimes A$ to itself. The LHS of the Figure represents

$$\begin{aligned} & (m \otimes m) \circ (1 \otimes P \otimes 1) \circ (\Delta \otimes \Delta)(a \otimes b) \\ &= (m \otimes m) \circ (1 \otimes P \otimes 1)(\Delta a \otimes \Delta b) \\ &= (m \otimes m)(a_1 \otimes b_1 \otimes a_2 \otimes b_2) = (a_1 b_1) \otimes (a_2 b_2) \end{aligned}$$

while the RHS represents

$$\Delta \circ m(a \otimes b) = \Delta(ab) = (ab)_1 \otimes (ab)_2$$

and these are equal by the consistency condition between multiplication and comultiplication. This shows that the Hopf algebra structure gives solutions to the equation that corresponds to the cone move.

That the partition function in this case does not depend on the choice of triangulation is proved by showing that the Pachner moves follow from the cone move and other singular moves. Figure 18 explains why the $(2 \rightleftharpoons 3)$ -move follows from singular moves (this Figure is similar to a Figure in [14]).

Let us explain the Figure. The first polyhedron is the RHS of the $(2 \rightleftharpoons 3)$ -move. There are three internal faces and three tetrahedra. Perform the cone move along edge (25) thereby duplicating face (125). Internally, we have face (125) glued to face (235) along edge (25) and face (125)' glued to face (245) along edge (25)'. These faces are depicted in the second polyhedron. By associativity these faces can be replaced by four faces parallel to four faces on the boundary; (123), (135), (124), (145). This is the configuration in the third polyhedron. Then there are two 3-cells bounded by these parallel faces. Collapse these cells and push the internal faces onto the boundary (this is done by singular moves). The result is the fourth polytope which now is a single polytope without any internal faces. This is the middle stage in the sense that we have proved that the RHS of the $(2 \rightleftharpoons 3)$ -move is in fact equivalent to this polytope.

Now introduce a pair of internal faces parallel to the faces (135) and (145) to get the fifth polytope (the left bottom one). Perform associativity again to change it to a pair of faces (134) and (345) to get the sixth polytope. Perform a cone move along the pair of faces with vertices (345). (These faces share edges (35) and (45); edge (34) is duplicated.)

The last picture results from this move, and this is the LHS of the $(2 \rightleftharpoons 3)$ -move.

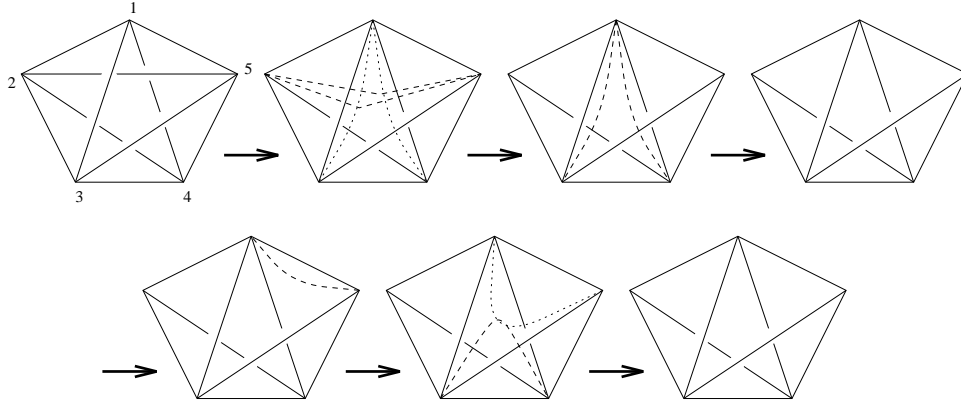


Figure 18: A Pachner move follows from cone moves

In summary, we perform cone moves and collapse some 3-cells to the boundary and prove that both sides of the Pachner move are, in fact, equivalent to the polyhedral 3-cell without internal faces. We give a generalization of this Theorem to dimension 4 in Section 5.5.

4.2.5 Biedenharn-Elliott revisited: the Turaev-Viro invariants. One way to view the Turaev-Viro invariants is to “categorify” the LTFT in dimension 2. In this process, the semi-simple algebra is replaced by a semi-simple monoidal category — namely the category of representations of $U_q(sl(2))$ where q is a primitive $4r$ th root of unity. First we review the definition of the Turaev-Viro invariants, and then explain the view point mentioned above.

A triangulation of a 3-manifold is given. A coloring, f , is *admissible* if edges with colors a, b, j bound a triangle, then the triple (a, b, j) is a q -*admissible triple* in the sense that

1. $a + b + j$ is an integer,
2. $a + b - j, b + j - a$, and $a + j - b$ are all ≥ 0
3. $a + b + j \leq r - 2$.

If edges with labels a, b, c, j, k, n are the edges of a tetrahedron such that each of (a, n, k) , (b, c, n) , (a, b, j) , and (c, j, k) is a q -admissible triple, then the tetrahedron, T , receives a weight of $T_f = \begin{bmatrix} a & b & n \\ c & k & j \end{bmatrix}_q$. This weight is a normalized quantum analogue of the $6j$ -symbol defined in Section 2. If any of these is not admissible, then the weight associated to a tetrahedron is, by definition, 0.

For a fixed coloring f of the edges of the triangulation of a 3-manifold M , the value

$$|M|_f = \Delta^{-t} \prod \Delta_{f(E)} \prod T_f$$

is associated where t is the number of vertices in the triangulation, the first product is taken over all the edges in the triangulation, the second product is over all the tetrahedra, the factor Δ is a normalization factor ($= \text{const.}$) and $\Delta_{f(E)}$ is a certain quantum integer associated to the color of the edge E . To obtain an invariant of the manifold one forms the sum

$$|M| = \sum_f |M|_f$$

where the sum is taken over all colorings. Further details can be found in [53, 31] or [12].

In Section 2.3 we reviewed the definition of $6j$ -symbols which involved two inclusions $V^k \rightarrow V^a \otimes V^b \otimes V^c$. These inclusions were constructed by taking two different groupings: $(V^a \otimes V^b) \otimes V^c$ and $V^a \otimes (V^b \otimes V^c)$. The pentagon relation, then, is regarded as the next order associativity condition.

This situation can be seen as a categorification. In 2-dimensions the associativity law $(ab)c = a(bc)$ played a key role. In 3-dimensions the $6j$ symbols are defined by comparing two different bracketings $(V^a \otimes V^b) \otimes V^c$ and $V^a \otimes (V^b \otimes V^c)$. Here the algebra elements became vector spaces as we went up the dimension by one, and the symbol measuring the difference in associativity satisfies the next order associativity, which in turn corresponds to the Pachner move.

4.3 Higher dimensions. In general, an n -dimensional Pachner move of type $(i \rightleftharpoons j)$, where $i + j = n + 2$, is obtained by decomposing the (spherical) boundary of an $(n + 1)$ -simplex into the union of two n -balls such that one of the balls is the union of i n -simplices, the other ball is the union of j n -simplices, and the intersection of these balls is an $(n - 1)$ -sphere. By labeling the vertices of the $(n + 1)$ -simplex these moves are easily expressed. For example, the table below indicates the lower dimensional Pachner moves:

$n = 1$	$(1 \rightleftharpoons 2)$	$(01) \rightleftharpoons (02) \cup (12)$
$n = 2$	$(1 \rightleftharpoons 3)$	$(012) \rightleftharpoons (013) \cup (023) \cup (123)$
	$(2 \rightleftharpoons 2)$	$(012) \cup (023) \rightleftharpoons (013) \cup (123)$
$n = 3$	$(1 \rightleftharpoons 4)$	$(0123) \rightleftharpoons (0134) \cup (0234) \cup (1234)$
	$(2 \rightleftharpoons 3)$	$(0123) \cup (1234) \rightleftharpoons (0124) \cup (0134) \cup (0234)$
$n = 4$	$(1 \rightleftharpoons 5)$	$(01234) \rightleftharpoons (01235) \cup (01245) \cup (01345) \cup (02345) \cup (12345)$
	$(2 \rightleftharpoons 4)$	$(01234) \cup (01235) \rightleftharpoons (12345) \cup (01245) \cup (01345) \cup (02345)$
	$(3 \rightleftharpoons 3)$	$(01234) \cup (01245) \cup (02345) \rightleftharpoons (01235) \cup (01345) \cup (12345)$

5 The Pachner Theorem in Dimension 4

In this lecture we examine in detail the 4-dimensional Pachner Theorem. First we give some motivation based on some constructions of Crane and Frenkel.

5.1 Crane-Frenkel invariants in dimension 4. Crane and Frenkel [15] proposed a construction of invariants of 4-manifolds using triangulations. We summarize their approach here before describing the Pachner moves in dimension 4 in detail. In fact theorems in the next section will be useful in studying invariants proposed by Crane and Frenkel, and our motivation was to provide a diagrammatic foundations for their approach, and other (yet to be found) combinatorial formulas for 4-manifold invariants.

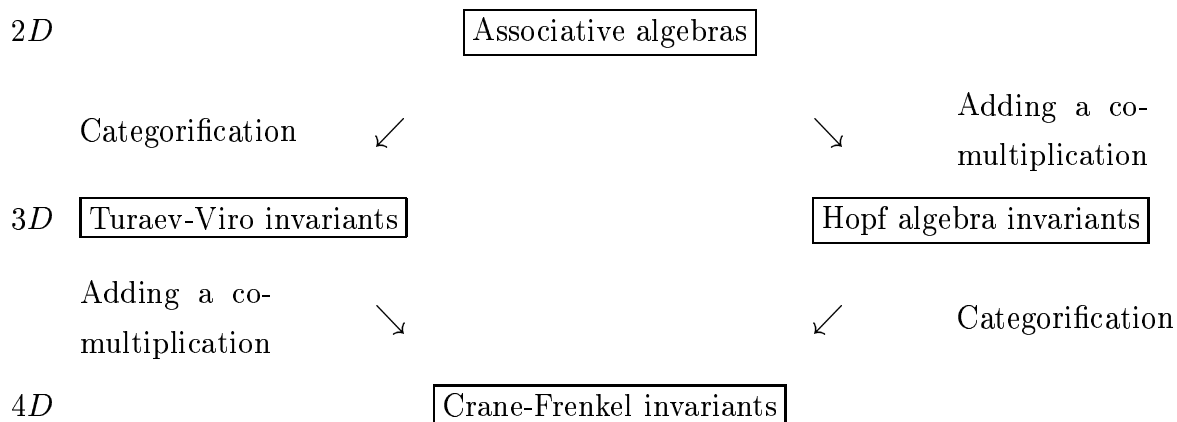
As we reviewed the invariants in dimensions 2 and 3, there are two ways to go up the dimension from 2 to 3. One way is to consider the algebras formed by representations of quantum groups as in Turaev-Viro invariants. In this case algebra elements are regarded as vector spaces (representations) and algebras are replaced by such categories. This process is called categorification. The second way is to include a comultiplication in addition to the multiplication of an algebra as in Hopf algebra invariants and consider bialgebras (in fact Hopf algebras) instead of algebras.

Let us explain these ideas in more details. Recall that in dimension 2 a Pachner move corresponds to associativity of algebras. If we consider a category of representations, it behaves like an algebra. Specifically, tensor product and direct sum together behaves like multiplication and addition of an algebra. In this context associativity is no longer an equality between elements, but it is a homomorphism between vector spaces. Here we are replacing elements by vector spaces. The $6j$ -symbols we discussed above is regarded as an associativity homomorphism. This in turn can be assigned to the movie of tree diagrams,

the dual of which is exactly a Pachner move in dimension 3. Thus we see here the idea that categorification corresponds to raising the dimension by one.

On the other hand, by introducing comultiplication, we were able to obtain new structural constants that can be assigned to edges of triangulations of 3-manifolds. Thus new algebraic operations can be used to go up the dimensions.

Crane and Frenkel defined invariants in dimension 4 using these ideas. They reach at the idea of the algebraic structure called *Hopf categories* either by (1) categorifying Hopf algebras, or (2) including comultiplications to categories of representations. The following chart represent this idea.



In the next section we study 4-dimensional Pachner moves in details. Our approach will provide combinatorial foundations for proving well-definedness of Crane-Frenkel invariants diagrammatically. Moreover, dual diagrams will provide direct relation between categorical structures and moves on triangulations.

5.2 4-dimensional Pachner Moves. One side of a 4-dimesional Pachner move is the union of 4-faces of a 5-simplex (homeomorphic to a 4-ball), and the other side of the move is the union of the rest of 4-faces.

In Figures 19 20, and 21 the $(3 \rightleftharpoons 3)$ -move, $(2 \rightleftharpoons 4)$ -move, and $(1 \rightleftharpoons 5)$ -move are depicted, respectively. Recall here that each 3-dimensional Pachner move represents a 4-simplex. Therefore the 3-dimensional Pachner move depicted in Figure 19 top left — the move represented by an arrow labeled (01234) — represents the 4-simplex with vertices 0, 1, 2, 3 and 4. Then the left-hand side of Figure 19 represents the union of three 4-simplicies $(01234) \cup (01245) \cup (02345)$. Similarly, the right-hand side of figure 19 represents the union of the three 4-simplicies $(01345) \cup (01235) \cup (12345)$.

5.3 The Stasheff Polytope. As we observed in Section 4, associativity is related to the 2-dimensional Pachner moves, and the pentagon relation involving parentheses structures

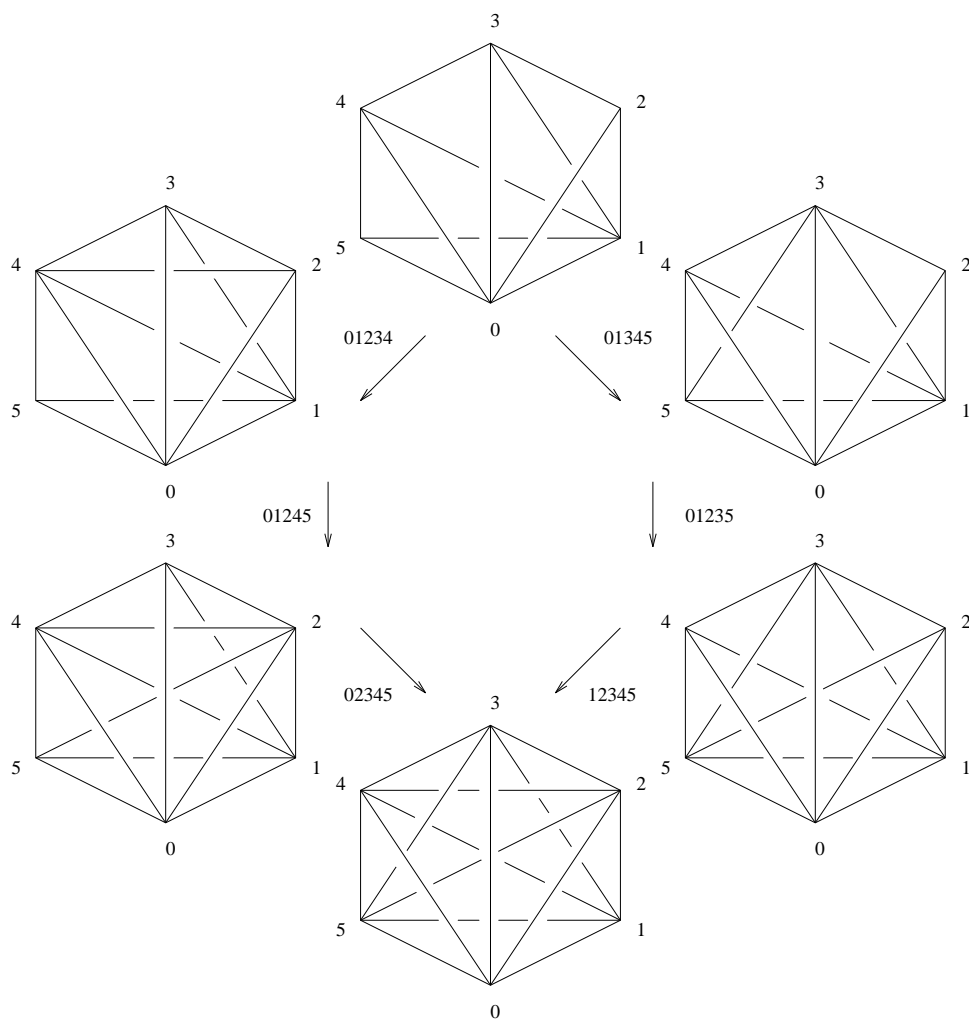


Figure 19: 4D Pachner move I

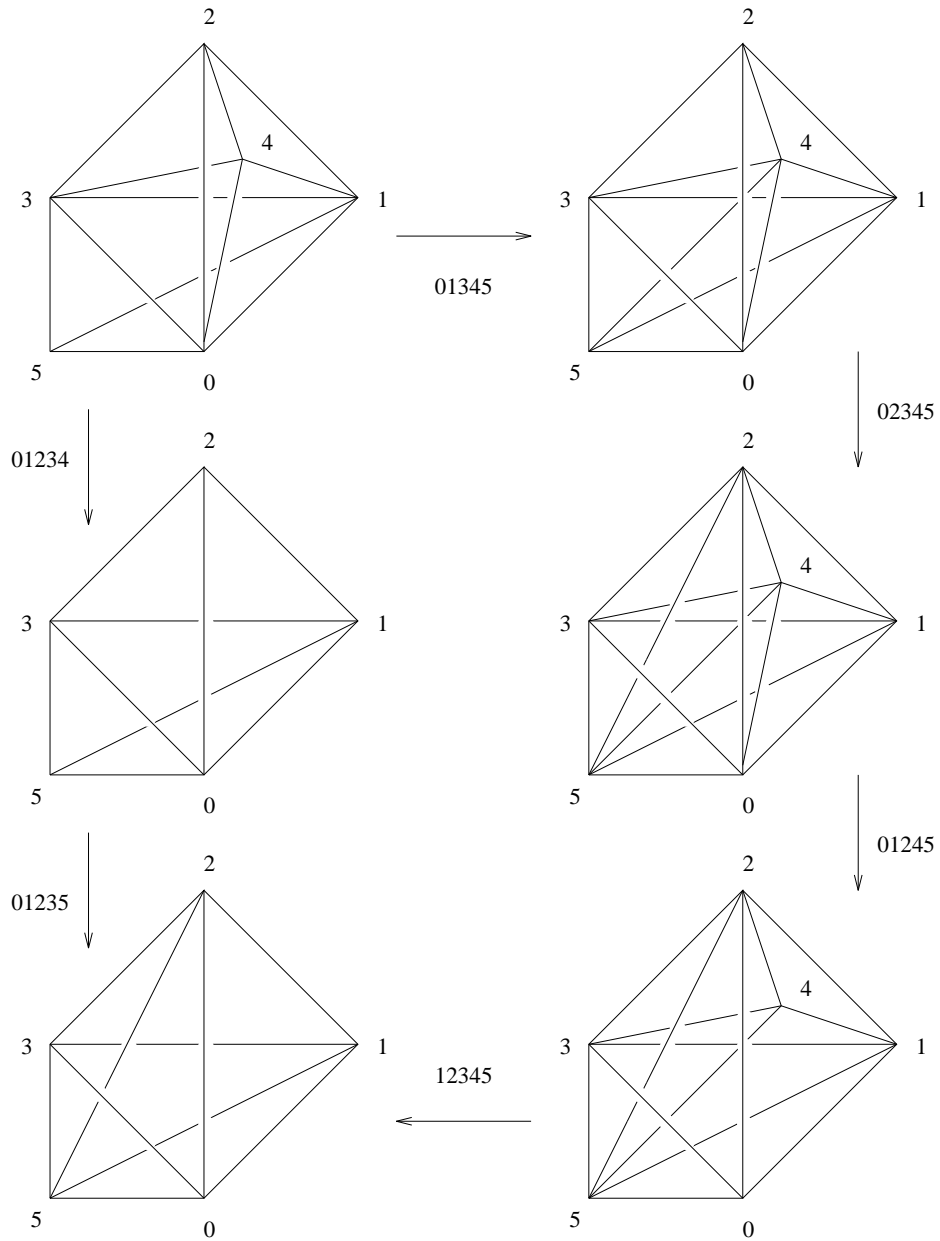


Figure 20: 4D Pachner move II

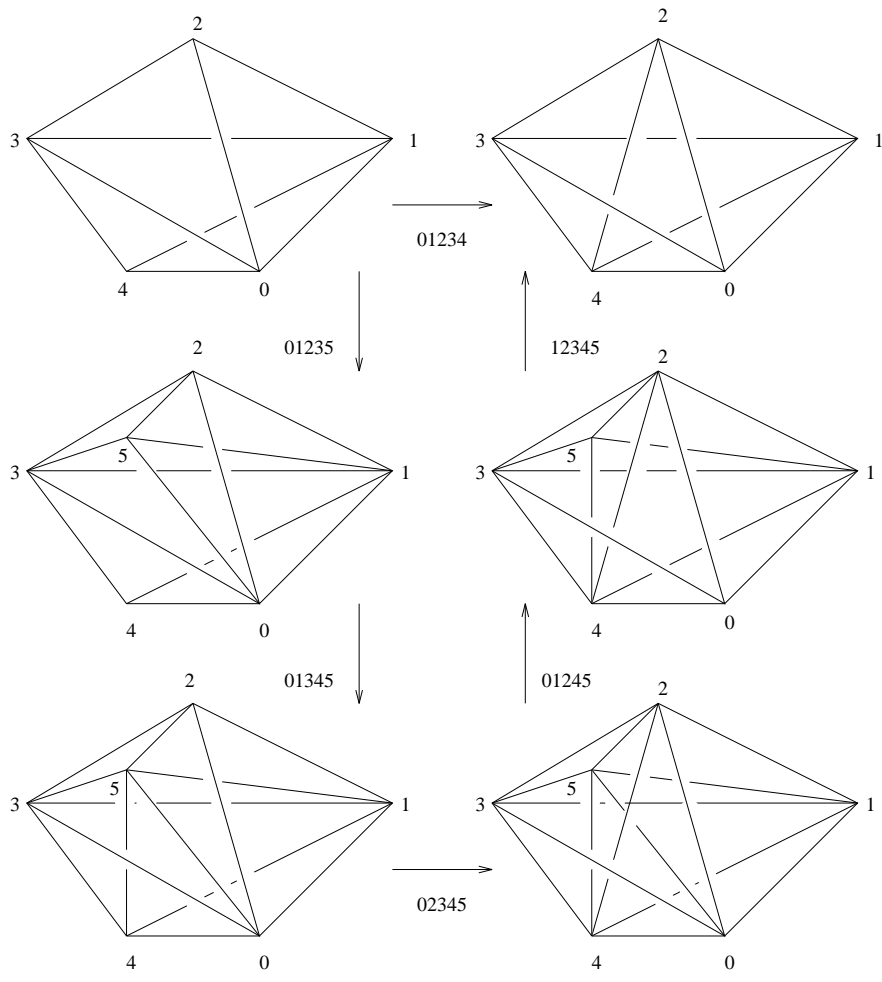


Figure 21: 4D Pachner move III

among four letters is related to 3-dimensional Pachner moves. The pentagon identity is regarded as second order associativity relation. The next order, the third order, associativity relation involving five letters is represented by a three dimensional polytope having vertices corresponding to parenthesis structures among five letters. This polytope and higher dimensional analogues were discovered by Jim Stasheff [50]. The 3-dimensional polyhedron is called *the -Stasheff polytope* or *the associahedron*. In this section we give explicit correspondences between Pachner moves in dimension 4 and the associahedron.

The 3-dimensional polytope is depicted in Figure 22, and its central projection through a quadrilateral face is shown in Figure 23. Figure 24 indicates the labeling of the vertices by triangulations of hexagons and their dual trees (indicated by dotted arcs).

The vertices of each in Figure 24 are labeled by triangulations of a hexagon. Consider, for example, the bottom pentagonal face of the associahedron. Each vertex of this pentagon is labeled by a hexagon in which the top triangle is fixed. Similarly, the left most pentagon has the southeast triangle fixed at its vertices. Thus each pentagon corresponds to a 4-face of the 5-simplex.

In Figure 25 the left-hand side of the $(3 \rightleftharpoons 3)$ Pachner move is depicted along the left column. The first row of the figure represents an edge path in the Stasheff polytope that starts from the middle-left vertex of Figure 24 and ends on the middle right vertex. To move to the next row, the edge path passes through the pentagonal face on the lower left of the center of Figure 24. This pentagon corresponds to the 4-face (01234). To get to the next row, the edge path slides over the quadrilateral on the lower right. Both of these edge paths represent the polytope on the second row of Figure 25; the homotopy between them represents the fact that the two tetrahedra (1234) and (0145) are glued along the edge (24), and they can be added to the polytope in either order. The edge path represented on the third row of Figure 25 has two edges on the bottom pentagon of Figure 24. The fourth row then is obtained from the third row by sliding across the bottom pentagon which corresponds to the 4-face (01245). The fifth row of Figure 24 is obtained from the fourth row by sliding the edge path across the left pentagon which corresponds to the 4-face (02345). The last row is obtained by sliding across the outside quadrilateral face.

The right side of the $(3 \rightleftharpoons 3)$ -move can be obtained similarly, by sliding the initial (zig-zag) edge path first across the upper-right center pentagon (01345), then across the upper left quadrilateral, across the upper pentagon (01235), and finally across the right pentagon (12345).

We can depict these sequences of edge paths as follows. First, number the vertices of the hexagons in Fig. 24 so that the bottom most vertex of each hexagon is labeled 0 and the labels increase in a counter-clock wise direction. The edges of the figure can then be labeled with quadruples of integers that indicate the quadrilateral on which the change in association is made. For example, the vertical edges on the outside of the figure are labeled (2345) while the horizontals are labeled (0125). The edge path described two paragraphs above is the following:

$$\begin{aligned}
& (0123)(0134)(0145) \\
\rightarrow & (0234)(0124)(1234)(0145) \\
\rightarrow & (0234)(0124)(0145)(1234) \\
\rightarrow & (0234)(0245)(0125)(1245)(1234) \\
\rightarrow & (0345)(0235)(2345)(0125)(1245)(1234) \\
\rightarrow & (0345)(0235)(0125)(2345)(1245)(1234)
\end{aligned}$$

The right hand side of the $(3 \rightleftharpoons 3)$ -move is the following sequence of edge paths.

$$\begin{aligned}
& (0123)(0134)(0145) \\
\rightarrow & (0123)(0345)(0135)(1345) \\
\rightarrow & (0345)(0123)(0135)(1345) \\
\rightarrow & (0345)(0235)(0125)(1235)(1345) \\
\rightarrow & (0345)(0235)(0125)(2345)(1245)(1234)
\end{aligned}$$

Each triangulated polytope of Figure 20 21 also corresponds to an edge path in the associahedron. Specifically, the LHS of $(2 \rightleftharpoons 4)$, $(01234) \cup (01235)$, corresponds to the homotopy of edge paths starting at the vertex of the associahedron labeled by the parenthesis $((a(bc)d)e$ and ending at $a((bc)(de))$

$$\begin{aligned}
& (0345)^{-1}(0234)(0124)(1234)(0134)^{-1}(0345)(0135) \\
\rightarrow & (0345)^{-1}(0123)(0345)(0135) \\
& \rightarrow (0123)(0135) \\
& \rightarrow (0235)(0125)(1235)
\end{aligned}$$

Here, we have to travel some edges against their orientation (in the above example (0345)) and such case is denoted by the inverse $((0345)^{-1})$. If an edge and its inverse appear in a sequence, then the corresponding tetrahedron does not appear in the polytope in Figure 20. This convention also applies to Figure 21.

The RHS of $(2 \rightleftharpoons 4)$ -move is represented by the sequence of edge paths:

$$\begin{aligned}
& (0345)^{-1}(0234)(0124)(1234)(0134)^{-1}(0345)(0135) \\
& \rightarrow (0345)^{-1}(0234)(0124)(1234)(0145)(1345)^{-1} \\
& \rightarrow (0235)(2345)(0245)^{-1}(0124)(1234)(0145)(1345)^{-1} \\
& \rightarrow (0235)(2345)(0245)^{-1}(0124)(0145)(1234)(1345)^{-1} \\
& \quad \rightarrow (0235)(2345)(0125)(1245)(1234)(1345)^{-1} \\
& \quad \quad \rightarrow (0235)(2345)(0125)(2345)^{-1}(1235) \\
& \quad \quad \quad \rightarrow (0235)(0125)(1235)
\end{aligned}$$

The two sides of the $(1 \rightleftharpoons 5)$ -move are sequences of edge paths from $((ab)c)d)e$ to $(ab)(c(de))$, are respectively

$$(0123)(0134) \rightarrow (0234)(0124)(1234)$$

and

$$\begin{aligned}
& (0123)(0134) \\
& \rightarrow (0345)(0123)(0345)^{-1}(0134) \\
& \rightarrow (0345)(0235)(0125)(1235)(0135)^{-1}(0345)^{-1}(0134) \\
& \quad \rightarrow (0345)(0235)(0125)(1235)(1345)(0145)^{-1} \\
& \rightarrow (0234)(0245)(2345)^{-1}(0125)(1235)(1345)(0145)^{-1} \\
& \rightarrow (0234)(0245)(0125)(2345)^{-1}(1235)(1345)(0145)^{-1} \\
& \rightarrow (0234)(0124)(0145)(1245)^{-1}(2345)^{-1}(1235)(1345)(0145)^{-1} \\
& \quad \rightarrow (0234)(0124)(0145)(1234)(0145)^{-1} \\
& \quad \quad \rightarrow (0234)(0124)(1234)
\end{aligned}$$

Thus we see that the low dimensional Pachner moves are, in the sense that we have described, encoded by the low dimensional polytopes.

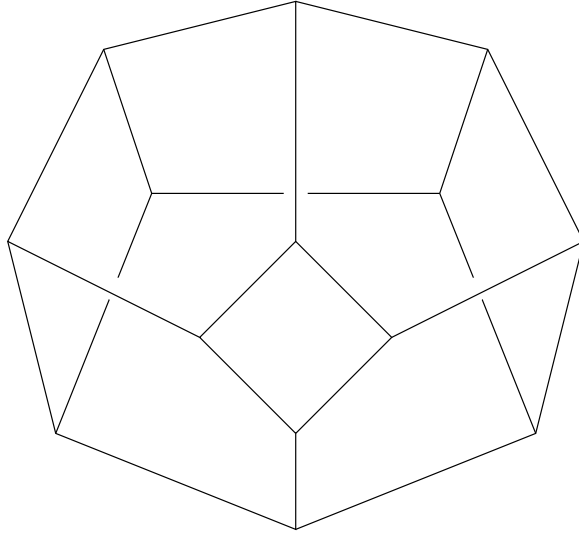


Figure 22: The Stasheff polytope

This correspondence between Stasheff polytopes and the Pachner moves also holds in all higher dimensions. Here we sketch the relationship; the reader is referred to [44], [22], and [23] for further details. In this paper we gave diagrams of 4D Pachner moves and more explicit and direct relations between the associahedron and the Pachner moves.

The vertices of the n -dimensional Stasheff polytope can be labeled by the triangulations of an $(n + 3)$ -gon where there are no internal vertices in the polygon. (As is well known, these triangulations are in one-to-one correspondence with parenthesized strings of letters a_1, \dots, a_{n+2} .) We think of a vertex of the Stasheff polytope as a 2-dimensional (aspherical) subcomplex of the $(n+2)$ -simplex. Each edge in the polytope can be labeled by a tetrahedron since each edge is a Pachner move of type $(2 \rightleftharpoons 2)$. So the edges correspond to tetrahedra. This pattern continues: The pentagonal faces correspond to 4-faces, *etc.*

5.3.1 Remark. Markl and Stasheff [39] used the associahedron for the study of obstruction cocycles to deformations of quasi Hopf algebras. In the light of Dikgraaf and Witten [17] invariants, such cocycles might be useful in defining invariants in dimension 4 using the relation between the associahedron and the 4-dimensional Pachner moves presented here.

5.4 Movies in the shadow world. The shadow method has been an effective means to understand and compute invariants of 3-dimensional manifolds. *The shadow of the dual spine to a tetrahedron* is a planar diagram that consists of either a 3-valent vertex or a

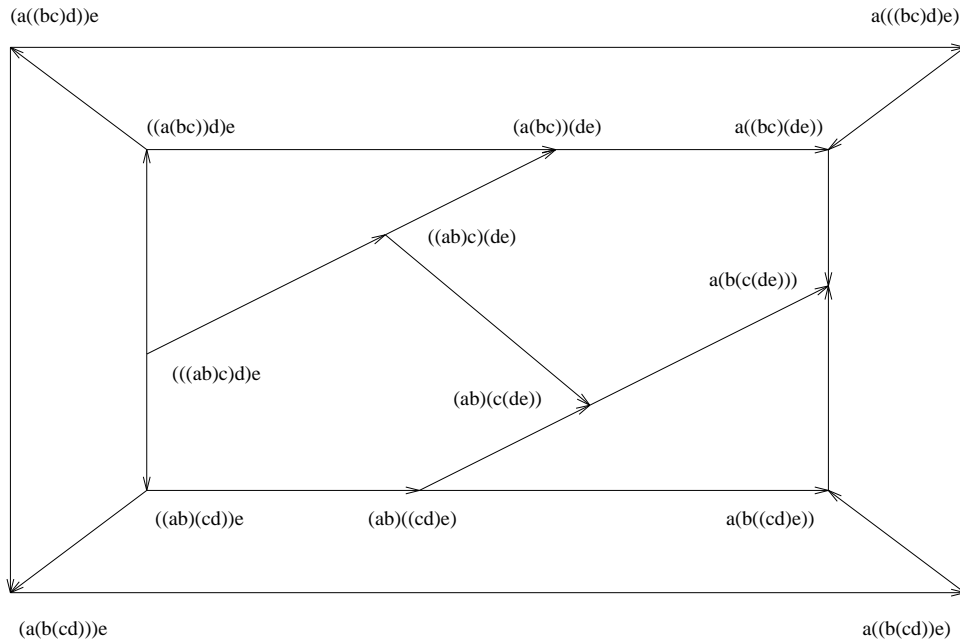


Figure 23: A projection of the Stasheff polytope (or the associahedron)

classical crossing from a knot diagram (thus a 4-valent vertex with crossing information). The shadow is the projection of the dual spine onto a union of 2-faces of the spine (see [52] for details). Figure 26 indicates the relationship among the tetrahedra, the spine, and its shadow. In the shadow model for the Turaev-Viro invariant, the colors are indicated on the edges and faces of the planar graphs. Thus the $6j$ -symbol that is associated to a colored tetrahedron in the Turaev-Viro model is denoted by a labeled planar diagram and many of the identities among $6j$ -symbols correspond to regular isotopies of these diagrams.

Since the $3D$ Pachner moves correspond to regular isotopies of planar graphs in the shadow world, the $4D$ Pachner moves correspond to relations between sequences of regular isotopies (we call these *shadow movies*) of planar graphs. In this section we present such sequences in the shadow world.

Figure 26 shows the labeling of planar graphs and regular isotopy of graphs corresponding to a Pachner move. In Figure 27 shadow movies are shown. Each of the vertices corresponds to some edge in the Stasheff polytope, each still in the shadow movie corresponds to an edge path, and each transformation between stills corresponds to sliding an edge path across one of the pentagonal faces of the polytope. We could include slides across the square faces as well, by including a height function on each still, and requiring that each vertex of a still lies at a different vertical level. The “shadow movie move” corresponds to the commutation

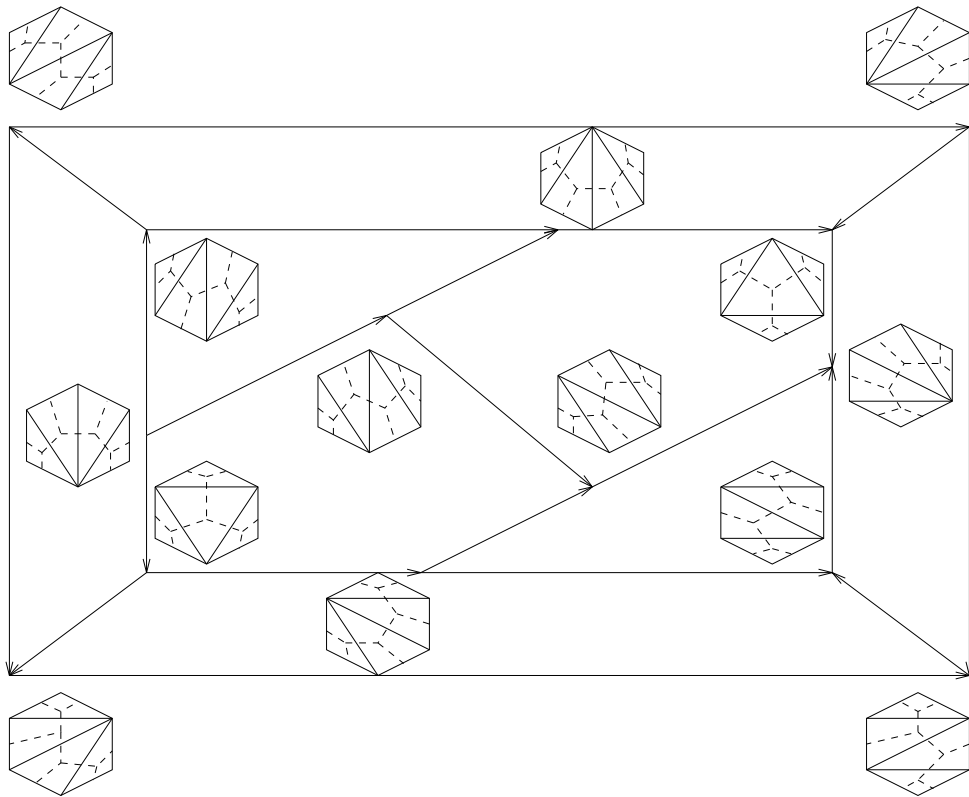


Figure 24: Polygons, trees, and the associahedron

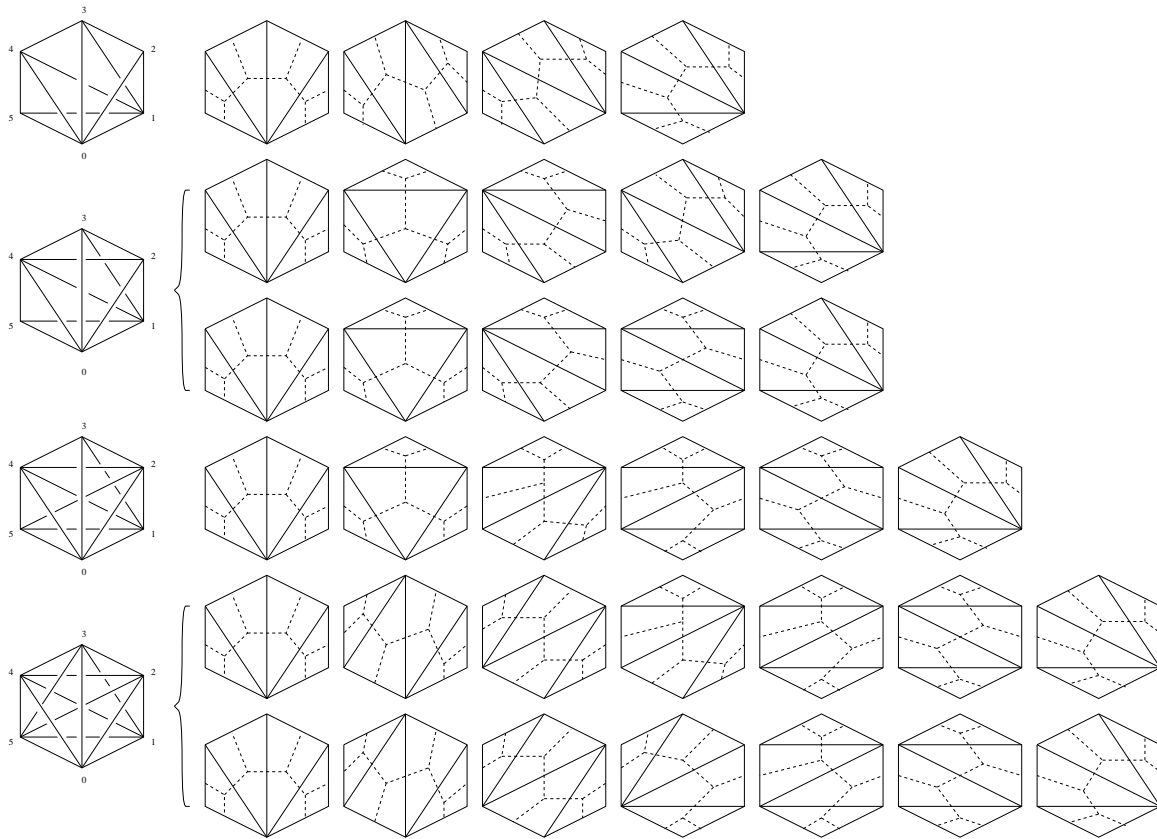


Figure 25: Paths in the Associahedron and a 4D dimensional Pachner move

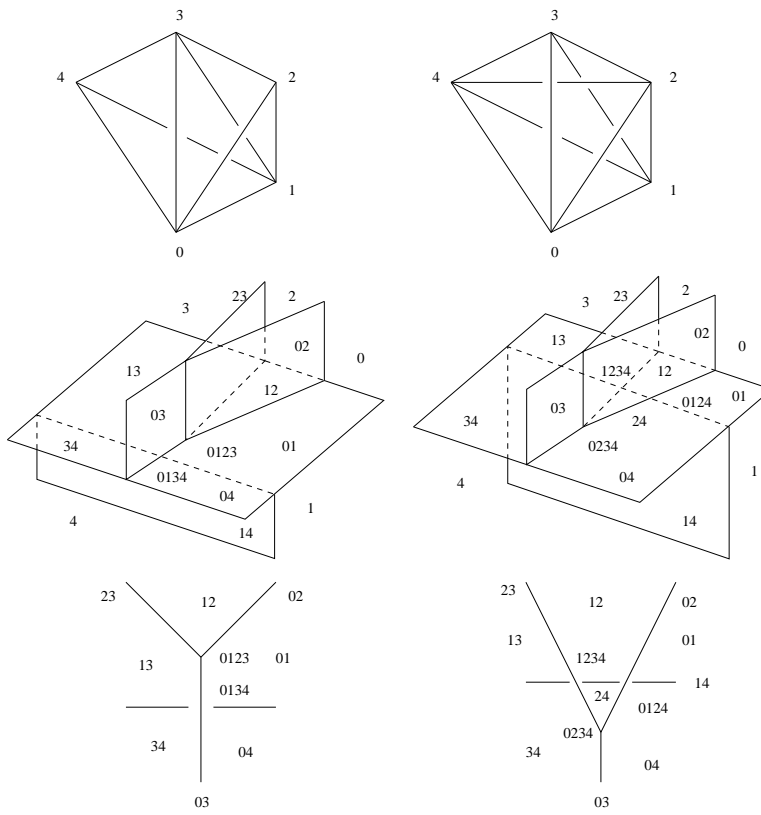


Figure 26: Dual complex and shadow labelings

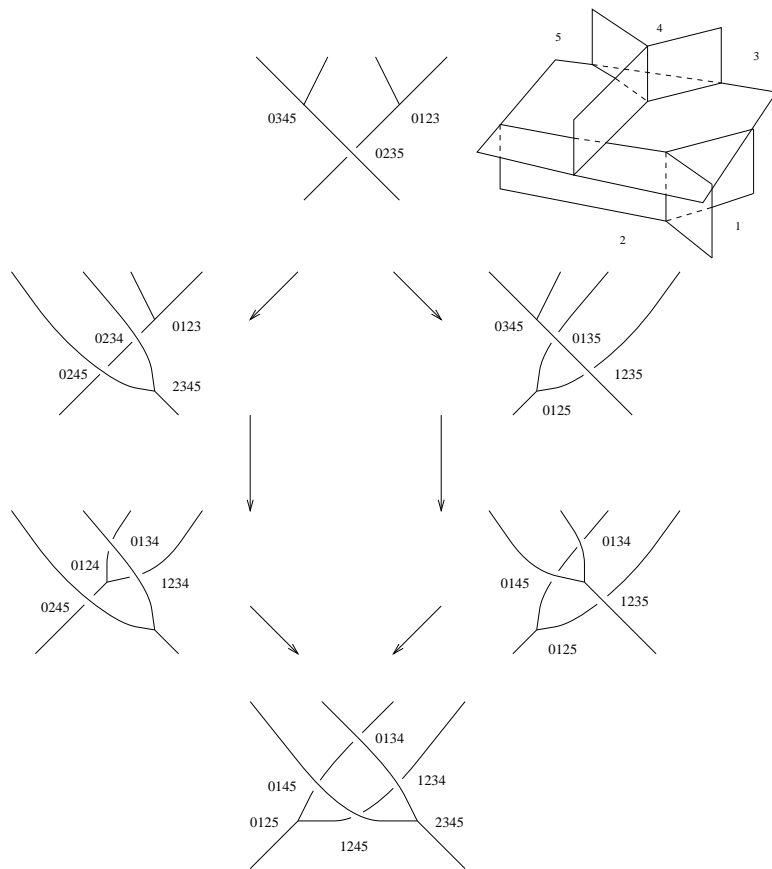


Figure 27: Shadow movies for a Pachner move

of the Stasheff polytope: A sequence of edge paths are related by sliding across faces of the polytope. Another sequence slide across the remaining faces.

One interpretation of these shadow movie moves is as follows. Imagine that the Y vertices in the stills represent a binary composition rule. Imagine further that the X represents a permutation. Then the top still in Fig. 27 represents the following sequence:

$$[a, b, c, d] \rightarrow [ab, cd] \rightarrow [cd, ab].$$

The left hand side of the movie move represents the following sequence of transformations:

$$\begin{aligned} & [a, b, c, d] \rightarrow [ab, cd] \rightarrow [cd, ab] \implies \\ & [a, b, c, d] \rightarrow [a, b, cd] \rightarrow [a, cd, b] \rightarrow [cd, a, b] \rightarrow [cd, ab] \implies \\ & [a, b, c, d] \rightarrow [a, c, b, d] \rightarrow [a, c, d, b] \rightarrow [a, cd, b] \rightarrow [cd, a, b] \rightarrow [cd, ab] \implies \\ & [a, b, c, d] \rightarrow [a, c, b, d] \rightarrow [c, a, d, b] \rightarrow [c, d, a, b] \rightarrow [cd, ab] \end{aligned}$$

The right hand side represents the following sequence of transformations:

$$\begin{aligned} & [a, b, c, d] \rightarrow [ab, cd] \rightarrow [cd, ab] \implies \\ & [a, b, c, d] \rightarrow [ab, c, d] \rightarrow [c, ab, d] \rightarrow [c, d, ab] \rightarrow [cd, ab] \implies \\ & [a, b, c, d] \rightarrow [a, c, b, d] \rightarrow [c, a, b, d] \rightarrow [c, ab, d] \rightarrow [c, d, ab] \rightarrow [cd, ab] \implies \\ & [a, b, c, d] \rightarrow [a, c, b, d] \rightarrow [c, a, d, b] \rightarrow [c, d, a, b] \rightarrow [cd, ab]. \end{aligned}$$

This case is reminiscent of the case of embedded surfaces. We have a sequence of words connected by a set of rules, and transformation rules between these sequences. The syzygies among the transformation rules require an algebraic interpretation.

5.5 Singular moves and Pachner moves. In dimension 4, the Pachner moves can be decomposed as singular moves and lower dimensional moves. Here we define a 4-dimensional cone move, and show how the Pachner moves follow.

5.5.1 Definition (cone move). The *cone move* for CW -complexes for 4-manifolds is defined as follows.

Suppose there is a pair of tetrahedra $(1234)_1$ and $(1234)_2$ sharing the same faces (123) , (124) and (134) , but have different faces $(234)_1$ and $(234)_2$, such that (1) $(234)_1$ and $(234)_2$ bound a 3-ball B in the 4-manifold, (2) the union of B , $(1234)_1$ and $(1234)_2$ is diffeomorphic to the 3-sphere bounding a 4-ball W in the 4-manifold.

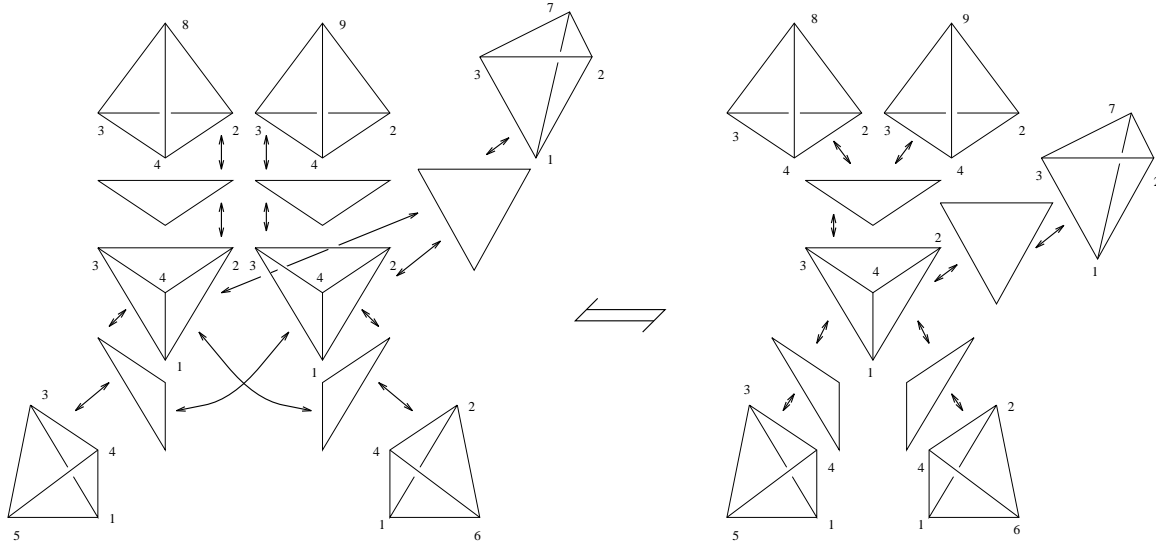


Figure 28: 4D cone move

The situation is depicted in Figure 28 which we now explain. The LHS of the Figure has two copies of tetrahedra with vertices 1, 2, 3, and 4. They share the same faces (123) , (124) , and (134) but have two different faces with vertices 2, 3, and 4.

The face $(234)_1$ is coincident to the tetrahedron (2348) while the face $(234)_2$ is coincident to (2349) . The face (123) (resp. (124) , (134)) is shared by $(1234)_1$, $(1234)_2$, and the tetrahedron (1237) (resp. (1246) , (1345)). Thus these faces are shared by three tetrahedra.

Collapse these two tetrahedra to a single tetrahedra to get the RHS of the Figure. Now we have a single tetrahedron with vertices 1, 2, 3, and 4. The face (234) now is shared by three tetrahedra (1234) , (2348) , and (2349) while three faces (123) , (124) , and (134) are shared by two tetrahedra.

5.5.2 Definition (taco move). Suppose we have a CW -complex such that there is a pair of tetrahedra $(0123)_1$ and $(0123)_2$ that share two faces (012) and (013) but have different faces $(023)_1$, $(023)_2$ and $(123)_1$, $(123)_2$ (of $(0123)_1$, $(0123)_2$ respectively). Suppose further that $(023)_1$, $(023)_2$, $(123)_1$, and $(123)_2$ together bound a 3-cell B and $(0123)_1$, $(0123)_2$, and B bounds a 4-cell. Then collapse this 4-cell to get a single tetrahedron (0123) . As a result $(023)_1$ (resp. $(123)_1$) and $(023)_2$ (resp. $(123)_2$) are identified. This move is called the *taco* move.

5.5.3 Definition (pillow move). Suppose we have a CW -complex such that there is a pair of tetrahedra sharing all four faces cobounding a 4-cell. Then collapse these tetrahedra to a single tetrahedron. This move is called the *pillow move*.

5.5.4 Lemma. *The $(3 \rightleftharpoons 3)$ Pachner move is described as a sequence of cone moves, pillow moves and Pachner moves.*

Proof. Before the proof we mention that the following arguments are obtained by looking at Fig. 19. We invite the reader to look at the Figure as s/he follows the proof. The left hand side of the $(3 \rightleftharpoons 3)$ -move consists of three 4-simplices $(01234) \cup (01245) \cup (02345)$. Denote this polytope by P . The 4-simplex (01245) has the tetrahedron (0245) as a 3-face. Split (0245) into two tetrahedra $(0245)_1$ and $(0245)_2$ by a cone move. Thus $(0245)_1$ and $(0245)_2$ share the same faces (025) , (045) and (245) but have different faces $(024)_1$ and $(024)_2$. The face $(024)_1$ is shared with (0124) and the face $(024)_2$ is shared with (0234) respectively.

After the splitting P consists of three 4-polytopes, τ_j^1 , $j = 1, 2, 3$. Here the polytope τ_1^1 is bounded by tetrahedra (0123) , (0134) , (0124) , (0234) , (1234) , $(0245)_1$, and $(0245)_2$. The polytope τ_2^1 is bounded by tetrahedra (0124) , (0145) , $(0245)_1$, (0125) , and (1245) . The polytope τ_3^1 is bounded by tetrahedra (0234) , $(0245)_2$, (0235) , (0345) , and (2345) . (The polytope τ_1^1 (resp. τ_2^1 , τ_3^1) corresponds to the 4-simplex (01234) (resp. (01245) , (02345) before the splitting.)

Next perform a Pachner move to the pair of tetrahedra $(0234) \cup (0245)_2$ sharing the face $(024)_2$. Note that these two tetrahedra are shared by τ_1^1 and τ_3^1 so that the Pachner move we perform does not affect τ_2^1 . Thus we get three 4-cells τ_j^2 , $j = 1, 2, 3$, where $\tau_2^2 = \tau_2^1$, and τ_1^2 is bounded by (0123) , (0134) , (0124) , (1234) , $(0245)_1$, $(0235)'$, $(0345)'$, and $(2345)'$. Here $(0235)'$, $(0345)'$, and $(2345)'$ denote new tetrahedra obtained as a result of performing a Pachner move to $(0234) \cup (0245)_2$. Then the last polytope τ_3^2 is bounded by $(0235)'$, $(0345)'$, and $(2345)'$ that are explained above, and (0235) , (0345) , (2345) that used to be faces of τ_3^1 .

Then we can collapse τ_3^2 to the tetrahedra (0235) , (0345) , (2345) as follows.

Now τ_3^2 is a 4-cell bounded by (0235) , (0345) , (2345) , $(0235)'$, $(0345)'$, and $(2345)'$. The faces are shared by these tetrahedra as follows. The faces (023) and (025) (resp. (034) and (045) , (234) and (245)) are shared by (0235) and $(0235)'$ (resp. (0345) and $(0345)'$, (2345) and $(2345)'$). The face (035) (resp. (345) , (235)) is shared by (0235) and (0345) (resp. (0345) and (2345) , (0235) and (2345)). The face $(035)'$ (resp. $(345)'$, $(235)'$) is shared by $(0235)'$ and $(0345)'$ (resp. $(0345)'$ and $(2345)'$, $(0235)'$ and $(2345)'$).

Then perform the taco move to the pair (2345) and $(2345)'$ that share two faces (234) and (245) . Then the faces (235) and $(235)'$, (345) and $(345)'$ are identified after the move

respectively. The result is a 4-cell bounded by (0235), (0345), (0235)', and (0345)'. (Precisely speaking these faces have new sharing faces so that we should use the different labelings but no confusion will occur here, so we continue to use the same labelings.) The faces (023), (025), and (235) (resp. (034), (045), and (345)) are shared by (0235) and (0235)' (resp. (0345) and (0345)'). The face (035) (resp. (035)') is shared by (0235) and (0235)' (resp. (0345) and (0345)').

The cone move to (0345) and (0345)' followed by the pillow move to (0235) and (0235)' collapses τ_3^2 to $(0235) \cup (0345) \cup (2345)$ as claimed.

Thus we get two polytopes τ_1^2 and τ_2^2 . Next perform a Pachner move to $(0124) \cup (0245)_1$ which shares $(024)_1$. As a result we get three new tetrahedra $(0145)' \cup (0125)' \cup (1245)'$.

Thus we obtain τ_1^3 bounded by (0123), (0134), (1234), (0235), (0345), (2345), (0145)', (0125)', and (1245)', and τ_2^3 bounded by (0145), (0125), (1245), and $(0145)' \cup (0125)' \cup (1245)'$.

Hence we now can collapse τ_2^3 to the tetrahedra (0145), (0125), and (1245) in the same manner as we did to τ_3^2 . The result is a single polytope τ^4 resulted from τ_1^3 which has the same boundary tetrahedra as those of the left hand side of the 4D Pachner move. The same argument applies to the right hand side (because of symmetry) to get the same single polytope. This proves that $(3 \rightleftharpoons 3)$ -move is described as a sequence of singular moves (cone moves) and Pachner moves. \square

5.5.5 Lemma. *The $(2 \rightleftharpoons 4)$ -move is described as a sequence of cone moves, pillow moves, and Pachner moves.*

Proof. We use the following labeling for the $(2 \rightleftharpoons 4)$ -move in this proof:

$$(01234) \cup (01245) \rightleftharpoons (01235) \cup (01345) \cup (02345) \cup (12345).$$

Perform $(3 \rightleftharpoons 3)$ -move (which was proved to be a sequence of the singular moves in the preceding Lemma) to $(01235) \cup (01345) \cup (02345)$ to get $(01234)' \cup (01245)' \cup (02345)'$. Then the polytope now consists of $(01234)'$, $(01245)'$, $(02345)'$, and (02345) .

Perform a Pachner move to the tetrahedra $(0235) \cup (0345) \cup (2345)$, that are shared by $(02345)'$ and (02345) , to get $(0234) \cup (0245)'$.

This changes $(02345)' \cup (02345)$ to a 4-cell bounded by (0234), $(0234)'$, (0245) , and $(0245)'$. The cone move followed by the pillow move collapses this polytope yielding $(01234) \cup (01245)$, the LHS of the $(2 \rightleftharpoons 4)$ -move. \square

5.5.6 Lemma. *The $(1 \rightleftharpoons 5)$ -move is described as a sequence of cone moves, pillow moves, and Pachner moves.*

Proof. We use the following labelings:

$$(01234) \rightleftharpoons (01235) \cup (01245) \cup (01345) \cup (02345) \cup (12345).$$

Perform the $(2 \rightleftharpoons 4)$ -move to $(01235) \cup (01345) \cup (12345)$ to get $(01234) \cup (01245)' \cup (02345)'$.

The 4-simplices (02345) and $(02345)'$ share all the face tetrahedra except (0345) (and $(0345)'$). Perform a $(1 \rightleftharpoons 3)$ -move to these tetrahedra shared to get 4-cells bounded by copies of (0345) sharing all the 2-faces. Thus the pillow moves will collapse (02345) and $(02345)'$. The same argument collapses $(01245) \cup (01245)'$ to get the LHS of the $(1 \rightleftharpoons 5)$ -move. \square

5.5.7 Remark. In [15] Crane and Frenkel proposed constructions of 4-manifold quantum invariants using Hopf categories. Hopf categories generalize the definition of Hopf algebra to a categorical setting in the same way that modular categories generalize modules. One of the conditions in their definition is called the coherence cube which generalizes the compatibility condition of Hopf algebras between multiplication and comultiplication. They showed that this condition corresponds to the cone move. Thus Lemmas in this section can be used to prove the well-definedness of invariants they proposed by showing that their definition is invariant under Pachner moves.

5.6 Conclusion. In dimension 4, we have various analogues of the 2- and 3-dimensional structures occurring at the topological level. The topology suggests the content of the next order algebraic structure. For example, in the movies of the shadow world we were able to interpret the moves to spines as relations among the operations on parentheses. Alternatively, these are homotopies of paths in the Stasheff polyhedron, and all of the Pachner moves are interpreted thus. Moreover we can recover the polyhedron by means of the movies of the tree diagrams, and the singularities in these movies correspond to the faces of the polytope. Also, the concept of singular triangulations allows us to interpret the Pachner moves in terms of a lower dimensional move, and a collection of singular moves. This phenomenon occurs in the lower dimensions. The $(2 \rightleftharpoons 3)$ -move follows from associativity and a cone move; the $(1 \rightleftharpoons 3)$ -move follows from the associativity law and the 2-dimensional bubble move. These singular moves give rise to other algebraic structures, and so one expects the cone moves in dimension 4 to give rise to new more esoteric structures as well.

6 Knotted Surfaces

The purpose of this lecture is to review algebraic and categorical interpretations of knot diagrams in dimension 4 recently developed in [13].

6.1 Knotted surface diagrams. Recall in Section 4, we discussed the charts of embedded surfaces in 3-space. In this section, we will generalize to consider the diagrams of knotted surfaces in 4-space. First, we review the definition of a knotted surface diagram and its chart.

6.1.1 Definition. Recall that a generic map from a 2-manifold to 3-space has embedded points, double point curves, isolated triple points, and branch points. A *knotted surface diagram* consists of a generic projection of the surface into 3-space together with *crossing information* (defined in the next two sentences) included along the image of the double and triple point manifolds. The sheet of the diagram that is further from the hyper-plane onto which the surface is projected is broken; that is, a small tubular neighborhood of the image of one of the sheets of the double decker manifold is removed from the surface F . At a triple point, this will mean that there is an indication of a top, middle, and bottom sheet. Knotted surface diagrams of surfaces are also called *broken surface diagrams*. See [11] for more details. The local pictures of knotted surface diagrams are depicted in Fig. 29. We may abuse notation and not make the distinction between the diagram and the projection of the knotted surface. In particular, the moves to diagrams will be drawn as moves to projections.

6.1.2 Definition. Let F be an embedded surface in 4-space, project F generically into 3-space and consider a further generic projection onto a plane called *the retinal plane*. The situation is an analogue of that for embedded surfaces, but now we also consider the double points, triple points, and branch points of the projection of the surface. As in the case considered in Section 3, we pick a vertical and horizontal direction in the retinal plane. The retinal plane is chosen so that it does not intersect the image of the surface F . The critical points in the vertical direction, cusps, and crossings of folds of the surface are those illustrated in Fig. 4. The multiple point sets also have critical points and these can also intersect the fold singularities; these critical phenomena are illustrated in Fig. 30.

For each non-critical value $y \in \mathbf{R}$, the inverse image of y in \mathbf{R}^3 intersects the broken surface diagram in a classical knot diagram. The horizontal axis in the retinal plane provides a height function for this diagram. For example, such a diagram is illustrated in Fig. 31.

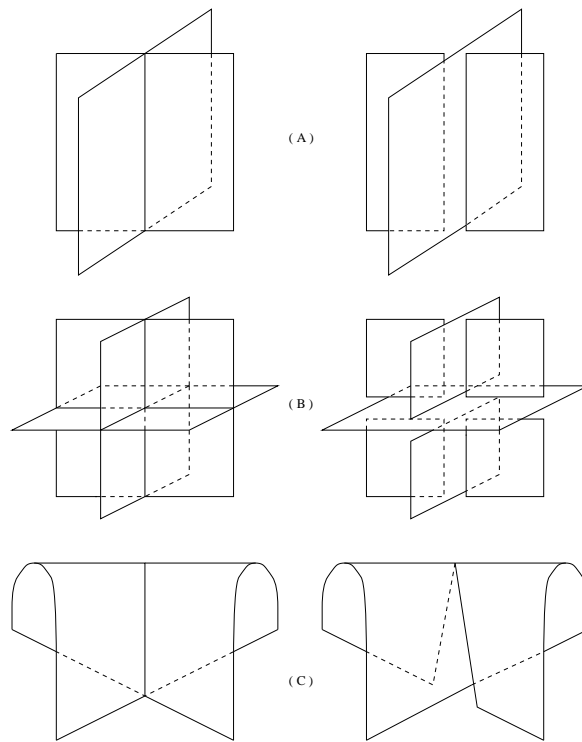


Figure 29: Projections and broken diagrams of knotted surfaces

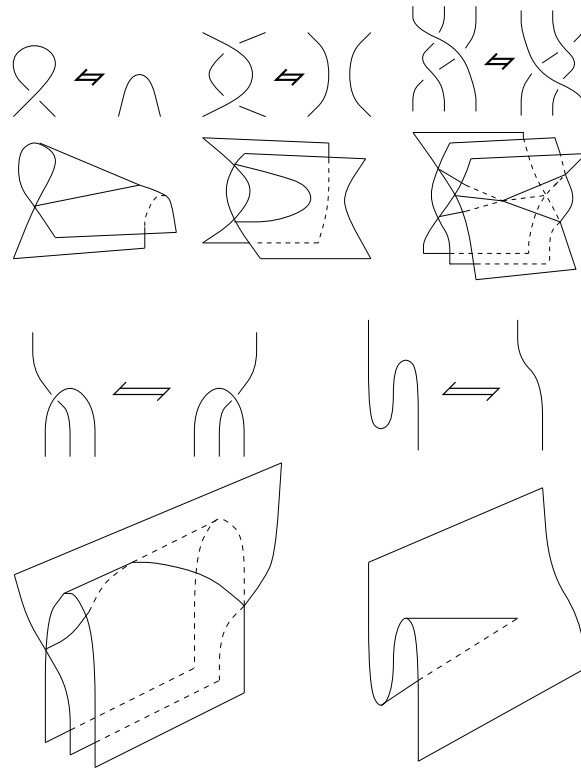


Figure 30: Critical points and crossing points of the self-intersection sets

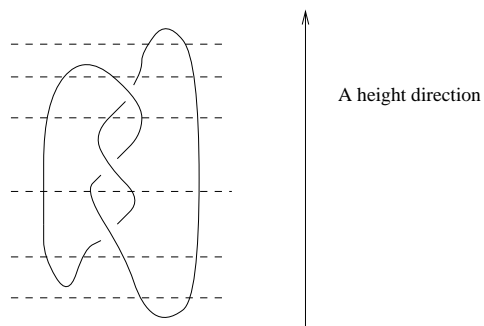


Figure 31: A knot diagram with a height function.

6.2 A combinatorial description of knotted surfaces. Next we study the planar projections of knotted surfaces diagrams to obtain a combinatorial description of knotted surfaces in terms of sequences of symbols.

6.2.1 Definition. Consider the image $\mathcal{I} = \pi \circ p \circ K(F)$ of a generic projection of a given knotted surface in the retinal plane. Let D denote the projections of the double points, triple points, and branch points considered as subsets of \mathcal{I} . Assume without loss of generality that the map $\pi \circ p \circ K$ is generic. Let S denote the image of the fold lines and cusps of the generic map $\pi \circ p \circ K$ in \mathcal{I} . Without loss of generality assume that D and S are in general position.

Let the *chart*, $C = C(K, p, \pi)$, of K with respect to p and π , be the planar graph $D \cup S$ considered as a subset of \mathcal{I} which is further contained in the retinal plane. We label the the chart C according to the following rules.

The image D is depicted by a collection of solid arcs while the image S is depicted by a collection of dotted arcs in our figures. In the figures a thick dotted arc can be either an arc in D or an arc in S .

There are seven types of vertices in the chart C ; these vertices correspond to isolated stable singularities of codimension 0.

(1) The projection of a triple point gives rise to a 6-valent vertex. Every edge among the six coming into the vertex is colored solidly.

(2) Each branch point in the projection of the knotted surface $K(F)$ corresponds to a 3-valent vertex. Two of the edges at the vertex are colored as dotted arcs (the fold lines); the other edge is solidly colored (the double arc that ends at the branch point).

(3) Each cusp of the projection π gives rise to a 2-valent vertex in which both edges are colored as dotted arcs.

(4) The projection of a point at which an arc of double point crosses a fold is a 4-valent vertex. Two of the edges at this vertex are solid; the other two are dotted. A circle in the retinal plane that encompasses such a vertex encounters the edges in the cyclic order (solid, solid, dotted, dotted).

(5) The points of the retinal plane at which the double points cross are 4-valent vertices at which all of the incoming edges are solid.

(6) The points of the retinal plane at which the fold lines cross are 4-valent vertices at which all of the incoming edges are dotted.

(7) The points of the retinal plane at which an arc of D crosses an arc of S are 4-valent vertices at which there are two solid edges and two dotted edges. A circle encompassing the vertex encounters the edges in cycle order (dotted, solid, dotted, solid).

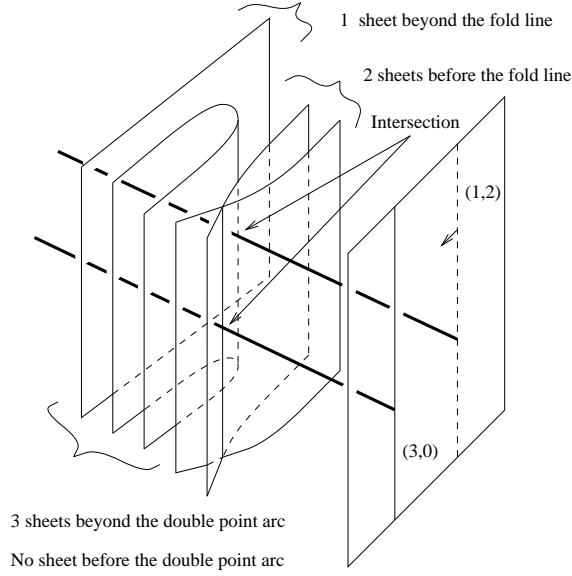


Figure 32: Labeling of charts

We use the projection of the knotted surface K in 3-space to label the edges of the chart as follows. Consider a ray R that is perpendicular to the retinal plane. Assume that R is in general position with $p(K(F))$, and assume that the end of the ray lies on an edge E . The edge E is the image of the double point arc or a fold line of $p(K(F))$. Let E' be the preimage (either the double point arc or a fold line). Let m (resp. n) be the number of sheets of $p(K(F))$ that are farther away (resp. closer to) from the retinal plane than E' along the ray. Then the pair of the integers (m, n) is assigned to the edge E as a label. The label does not depend on the choice of point along the edge near which the ray R starts.

6.2.2 Extending the 2-category. We can use the height function in the horizontal direction to express each non-critical cross-sectional knot diagram as diagram as word in symbols $\cup_{m,n}$, $\cap_{m,n}$, $X_{m,n}$, and $\bar{X}_{m,n}$. For example, the diagram of the trefoil in Fig. 31 corresponds to the sequence of symbols

$$\cap_{0,0} \cap_{0,2} X_{1,1} X_{1,1} X_{1,1} \cup_{0,2} \cup_{0,0}.$$

By cutting the knotted surface diagram with non-critical slices we get a sequence of such symbols, and these can be interpreted in 2-categorical language as in Section 3. In fact for the categorical interpretation we need to include 1-morphisms corresponding to the braidings $X_{j,k}, \bar{X}_{j,k} : j+k+2 \rightarrow j+k+2$. Moreover, we will generalize the notion of a sentence to one in which additional transitions between words are allowed. These transitions are codified by

the critical values, crossings, and cusps in the vertical direction of the retinal plane. Each such critical value corresponds to one of the elementary changes that are illustrated in either Fig. 4 or in Fig. 30.

6.2.3 Definition. Let a set of symbols $X_{m,n}$, $\bar{X}_{m,n}$, $\cap_{m,n}$ or $\cup_{m,n}$ be given. Define *the initial number of a symbol*, $\iota(Y_{m,n})$, and *the terminal number of a symbol*, $\tau(Y_{m,n})$, (where $Y_{m,n}$ in one of the above symbols) as follows: $\iota(X_{m,n}) = \iota(\bar{X}_{m,n}) = \tau(X_{m,n}) = \tau(\bar{X}_{m,n}) = m + n + 2$, $\iota(\cap_{m,n}) = m + n$, $\tau(\cap_{m,n}) = m + n + 2$, $\iota(\cup_{m,n}) = m + n + 2$, $\tau(\cup_{m,n}) = m + n$.

A *word* is a sequence $Y_0 \cdots Y_k$ in symbols $Y_j = X_{m,n}$, $\bar{X}_{m,n}$, $\cap_{m,n}$ or $\cup_{m,n}$ where m and n are non-negative integers such that $\tau(Y_j) = \iota(Y_{j+1})$.

For a word $W = Y_0 \cdots Y_k$ with Y_0 and Y_k non-empty, $\tau(W)$ is defined by $\tau(Y_k)$ and $\iota(W)$ is defined by $\iota(Y_0)$.

The empty word is allowed as a word, and any given word need not involve all of the symbols. If a word is non-empty, then its first (resp. last) letter will be \cap_{00} (resp. \cup_{00}).

A *sentence* is a sequence (W_0, W_1, \dots, W_f) of words such that W_0 and W_f are the empty words, and for any $i = 0, \dots, f - 1$, W_{i+1} is obtained from W_i by performing one of the following changes.

1. Cancellation or creation of a pair of adjacent symbols $\cap_{m,n}\cup_{m,n}$ in the word.
2. Cancellation or creation of a pair of adjacent symbols $\cup_{m,n}\cap_{m,n}$ in the word, for appropriate values on m, n .
3. A replacement of $\cap_{m,n}X_{m,n}$ by $\cap_{m,n}$, or vice versa; a replacement of $\cap_{m,n}\bar{X}_{m,n}$ by $\cap_{m,n}$, or vice versa; a replacement of $X_{m,n}\cup_{m,n}$ by $\cup_{m,n}$, or vice versa; and a replacement of $\bar{X}_{m,n}\cup_{m,n}$ by $\cup_{m,n}$, or vice versa.
4. Cancellation or creation of a pair $X_{m,n}\bar{X}_{m,n}$ or $\bar{X}_{m,n}X_{m,n}$.
5. A replacement of one of the following:

$X_{m,n}X_{m+1,n-1}X_{m,n}$ by $X_{m+1,n-1}X_{m,n}X_{m+1,n-1}$ or vice versa,

$X_{m,n}X_{m+1,n-1}\bar{X}_{m,n}$ by $\bar{X}_{m+1,n-1}X_{m,n}X_{m+1,n-1}$ or vice versa,

$X_{m,n}\bar{X}_{m+1,n-1}\bar{X}_{m,n}$ by $\bar{X}_{m+1,n-1}\bar{X}_{m,n}X_{m+1,n-1}$ or vice versa,

$\bar{X}_{m,n}X_{m+1,n-1}X_{m,n}$ by $X_{m+1,n-1}X_{m,n}\bar{X}_{m+1,n-1}$ or vice versa,

$\bar{X}_{m,n}\bar{X}_{m+1,n-1}X_{m,n}$ by $X_{m+1,n-1}\bar{X}_{m,n}\bar{X}_{m+1,n-1}$ or vice versa, or

$\bar{X}_{m,n}\bar{X}_{m+1,n-1}\bar{X}_{m,n}$ by $\bar{X}_{m+1,n-1}\bar{X}_{m,n}\bar{X}_{m+1,n-1}$.

Note that these correspond to various crossing types of Reidemeister type III move.

6. A replacement of $\cap_{m,n} X_{m+1,n-1}$ by $\cap_{m+1,n-1} \bar{X}_{m,n}$, vice versa, or a replacement of $\cap_{m,n} \bar{X}_{m+1,n-1}$ by $\cap_{m+1,n-1} X_{m,n}$, or vice versa.

A replacement of $X_{m+1,n} \cup_{m,n}$ by $\bar{X}_{m,n+1} \cup_{m+1,n-1}$, vice versa, or a replacement of $\bar{X}_{m+1,n} \cup_{m,n}$ by $X_{m,n+1} \cup_{m+1,n-1}$, or vice versa.

7. Cancellation or creation of a pair $\cap_{m,n} \cup_{m+1,n-1}$ or $\cup_{m,n} \cap_{m+1,n-1}$.
8. A replacement of $Y_{n,m} Y_{i,j}$ by $Y_{i,j} Y_{n,m}$ where $Y_{n,m}$ denotes either $X_{n,m}$ or $\bar{X}_{n,m}$.
9. A replacement of $Y_{n,m} Y'_{i,j}$ by $Y'_{i,j} Y_{n,m}$ where Y and Y' are \cap or \cup . This in fact means the Items (9) through (16) in the generating 2-morphisms in Section 3.3. See also the remark in the Item (4) of the sentence equivalences in Section 3.4.

Thus any knotted surface diagram (with projection onto the vertical axis in the retinal plane) gives rise to a sentence. Conversely, given a sentence we can construct a knotted surface diagram: Each word gives a knot diagram, and each successive pair of words gives rise to a FESI. In summary we have proved

6.2.4 Theorem. *To any knotted surface diagram a sentence is assigned. For any sentence there is a knotted surface whose corresponding sentence is the given one.*

The question of when two sentences represent isotopic knotted surfaces can be answered by combinatorially interpreting codimension 1-singularities of mappings of surfaces into the plane. A complete statement of that combinatorial equivalence is found in [13]. The moves to sentences that generate knotted surface isotopies are analogous to, and include, the moves listed in Section 3.4. The charts of the unfoldings of the codimension 1 singularities in this case are illustrated in Figs.33,34,35, and 36.

6.2.5 Theorem. *Two charts with fixed height function of isotopic knotted surfaces are related by the moves depicted in Figure 33 through 36.*

In the illustrations, the dotted curves represent fold lines, and the solid curves represent the projection of double point arcs. The thick dotted lines are either double point arcs or fold lines. Strictly speaking, all of these arcs should be labeled as indicated in Fig. 32, for without labels the moves are ambiguous.

Here we give some examples of how the chart moves correspond to “movie moves.” In the sequel we will use many of these to show a certain example is un-knotted.

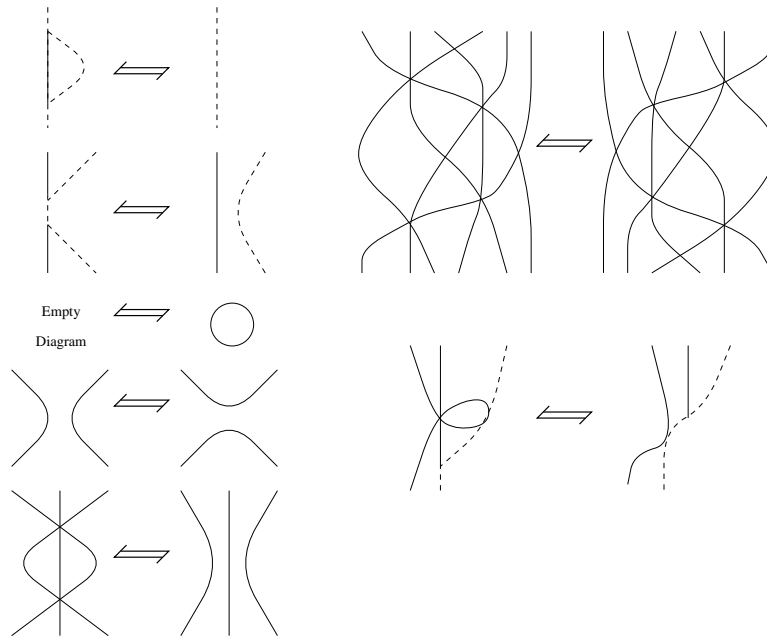


Figure 33: Chart moves, part I

6.3 Example. It was shown by Livingston and Boyle [37] [5] that the following example is unknotted. The example is known as the 1/3-turned trefoil. It is a torus embedded in 4-space in which there is a cross section consisting of a left hand a right hand trefoil. Here we indicate a movie of the surface, a chart, and a sequence of moves to charts that can be used to show the surface is unknotted. The charts can be expanded into film strips, and the entire calculation laided bare. The importance of this calculation is that it indicates that although one is manipulating diagrams, these diagrams could represent an algebraic expression. Moreover, once the appropriate algebraic expression is found that represents such diagrams, it seems clear that algebraic computation will be no more easy than diagrammatic manipulations.

6.4 Concluding remarks. In this paper we explored a remarkable feature of quantum topology: unexpected relations between diagrammatics and algebraic structures. We emphasized the viewpoint of identifying singularities with the relations in algebraic structures. We also presented new results on relations between the associahedron and the 4D Pachner moves given explicitly. We proved that the 4D Pachner moves follow from singular moves, utilizing our diagrams of 4D Pachner moves. We gave a review of new results on diagrammatics of knotted surfaces. Higher algebraic structures and 4D knots and manifolds deserve more

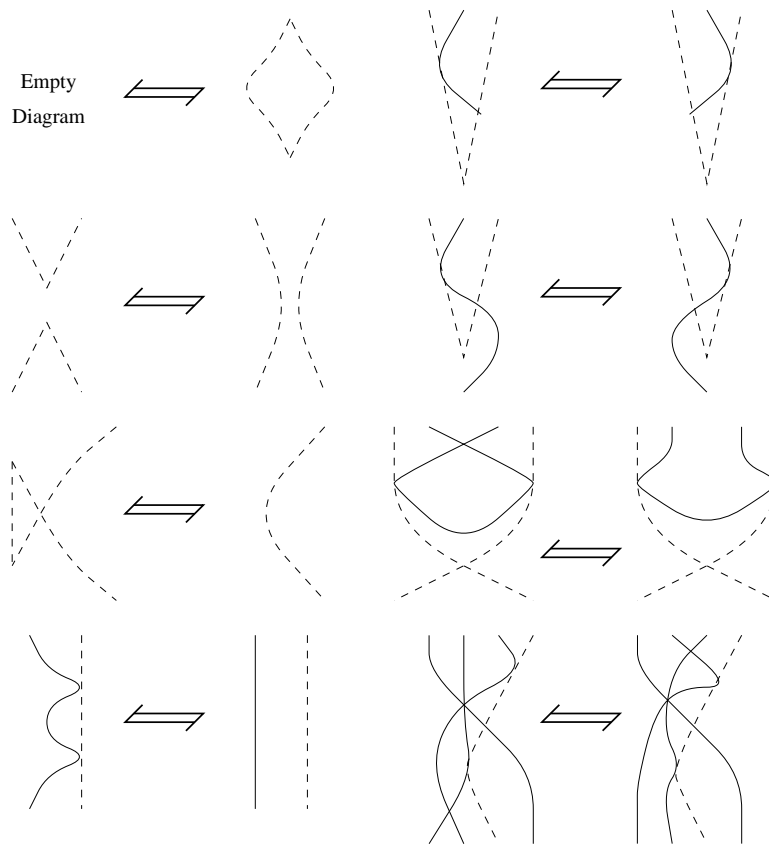


Figure 34: Chart moves, part II

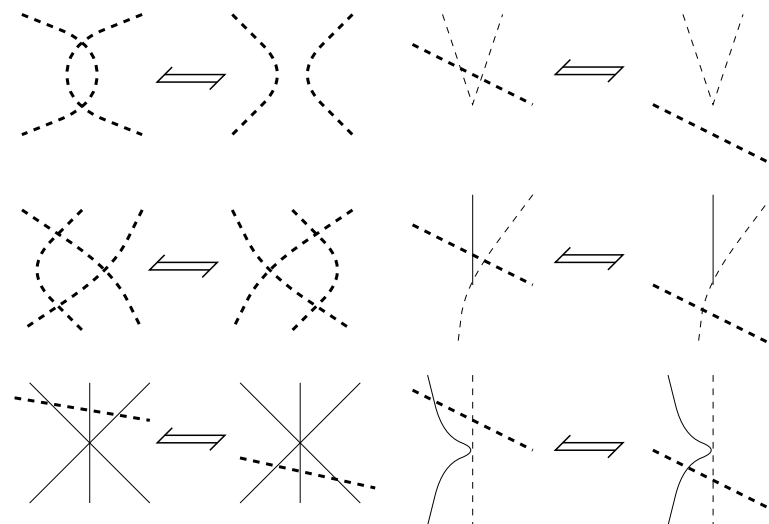


Figure 35: Chart moves, part III

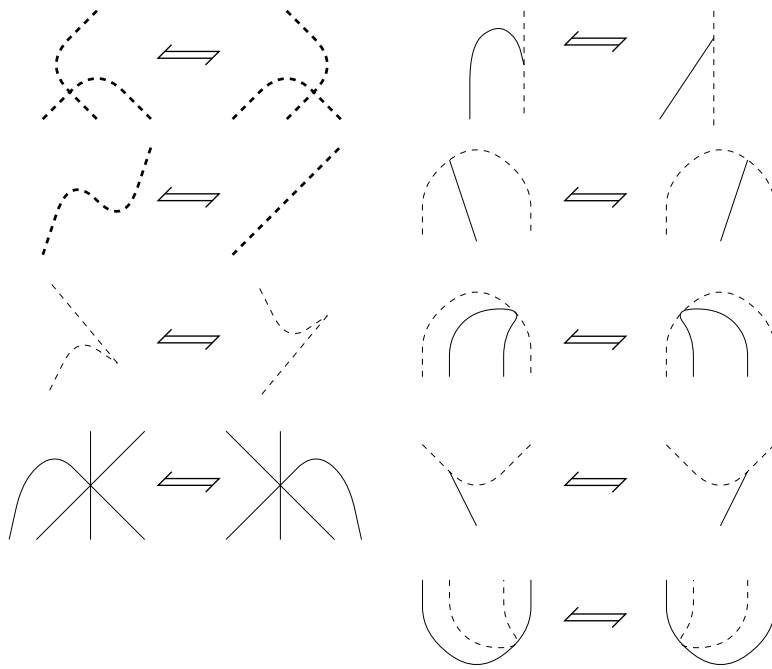


Figure 36: Chart moves, part IV

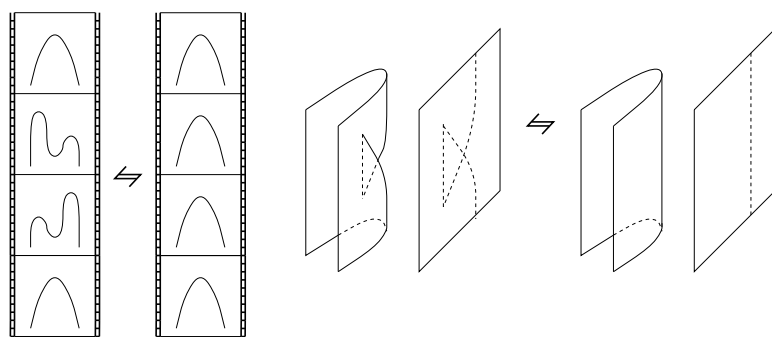


Figure 37: A swallow-tail on the fold lines

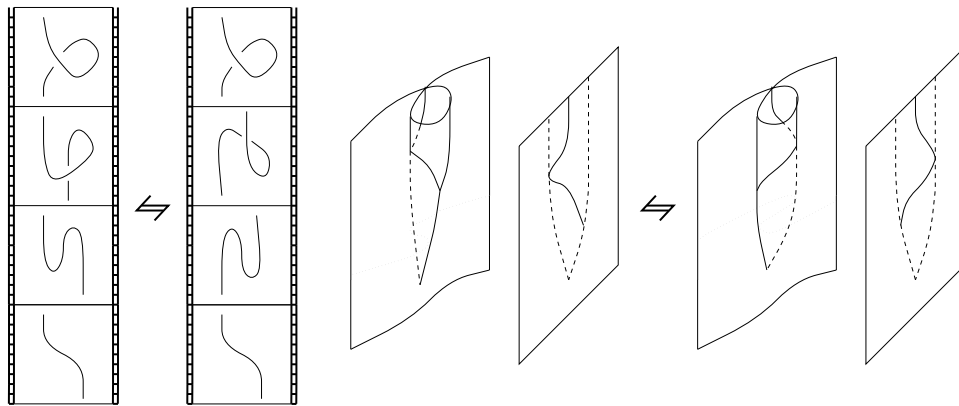


Figure 38: A branch point passes through a cusp

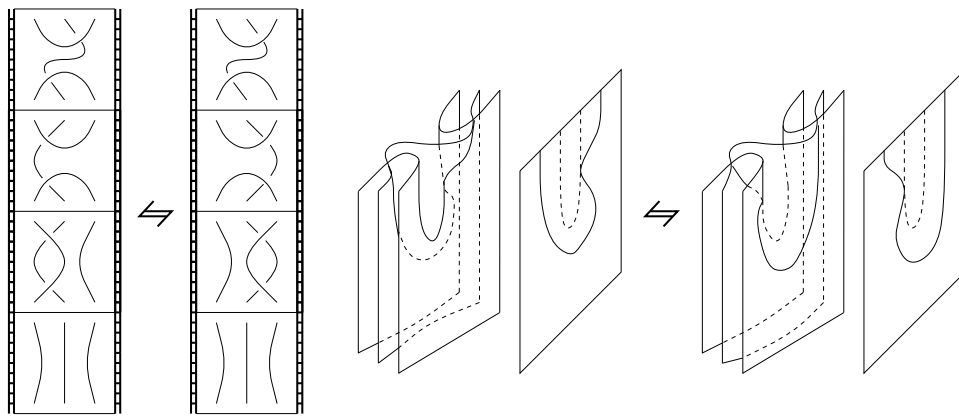


Figure 39: A double point arc passes over a fold line near a saddle point

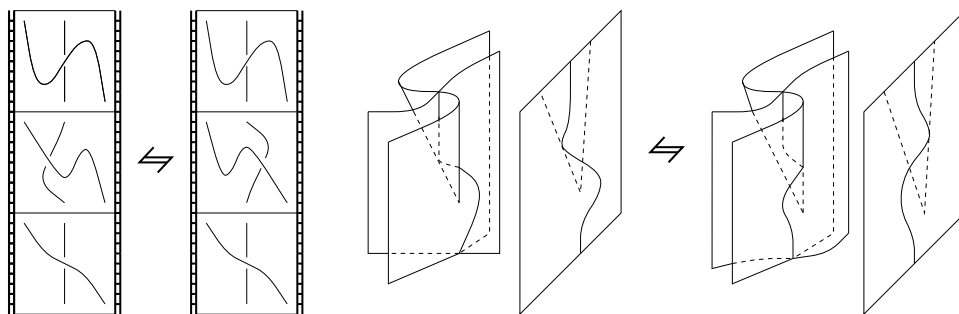


Figure 40: A double arc passes over a fold line near a cusp

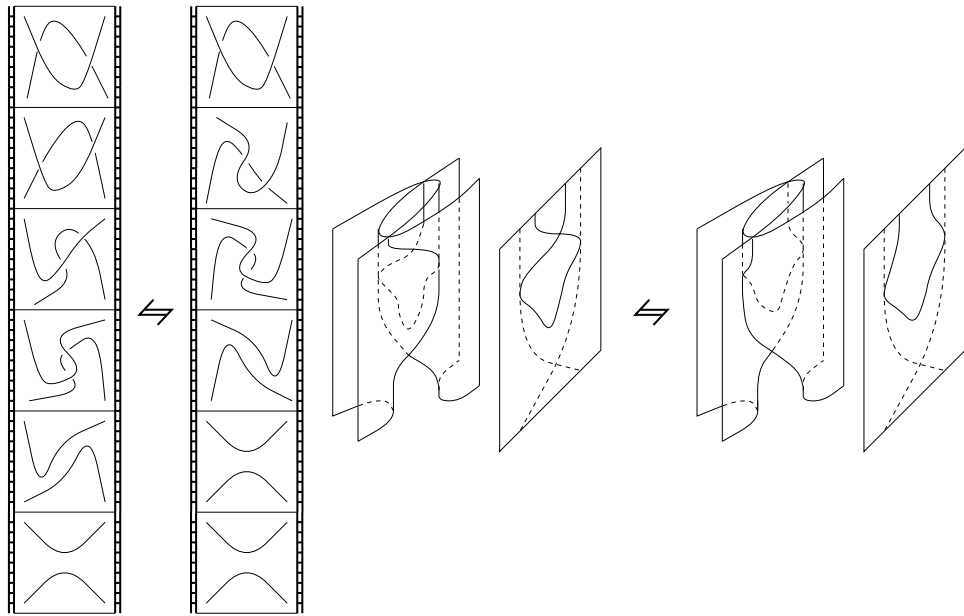


Figure 41: A double point arc becomes tangent to the line of projection

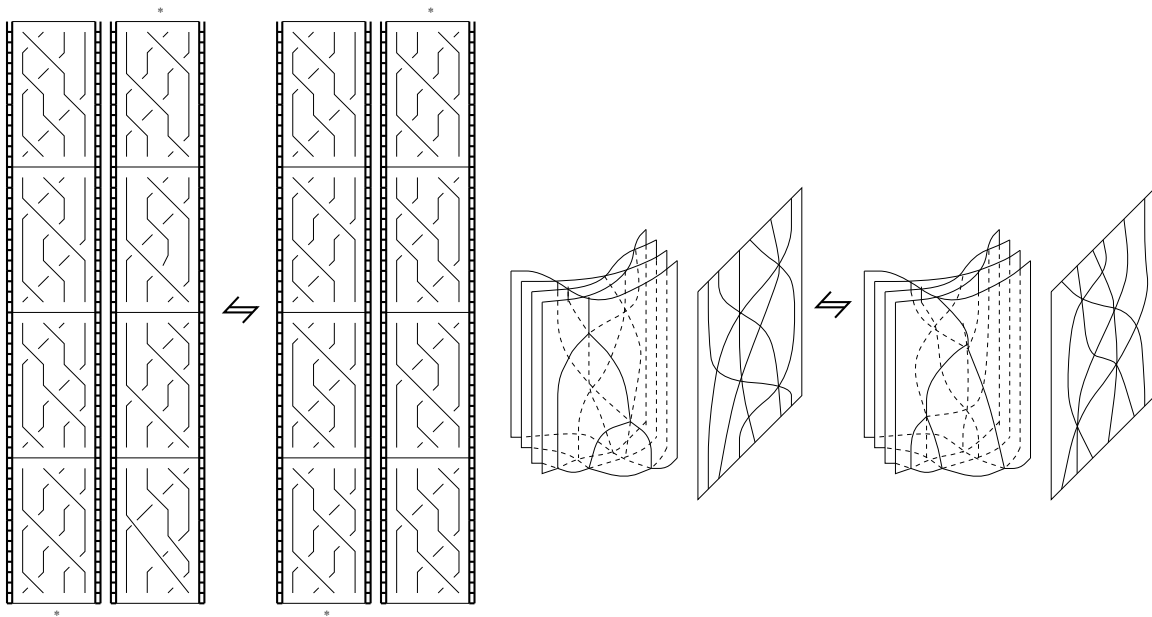


Figure 42: A quadruple point in the isotopy

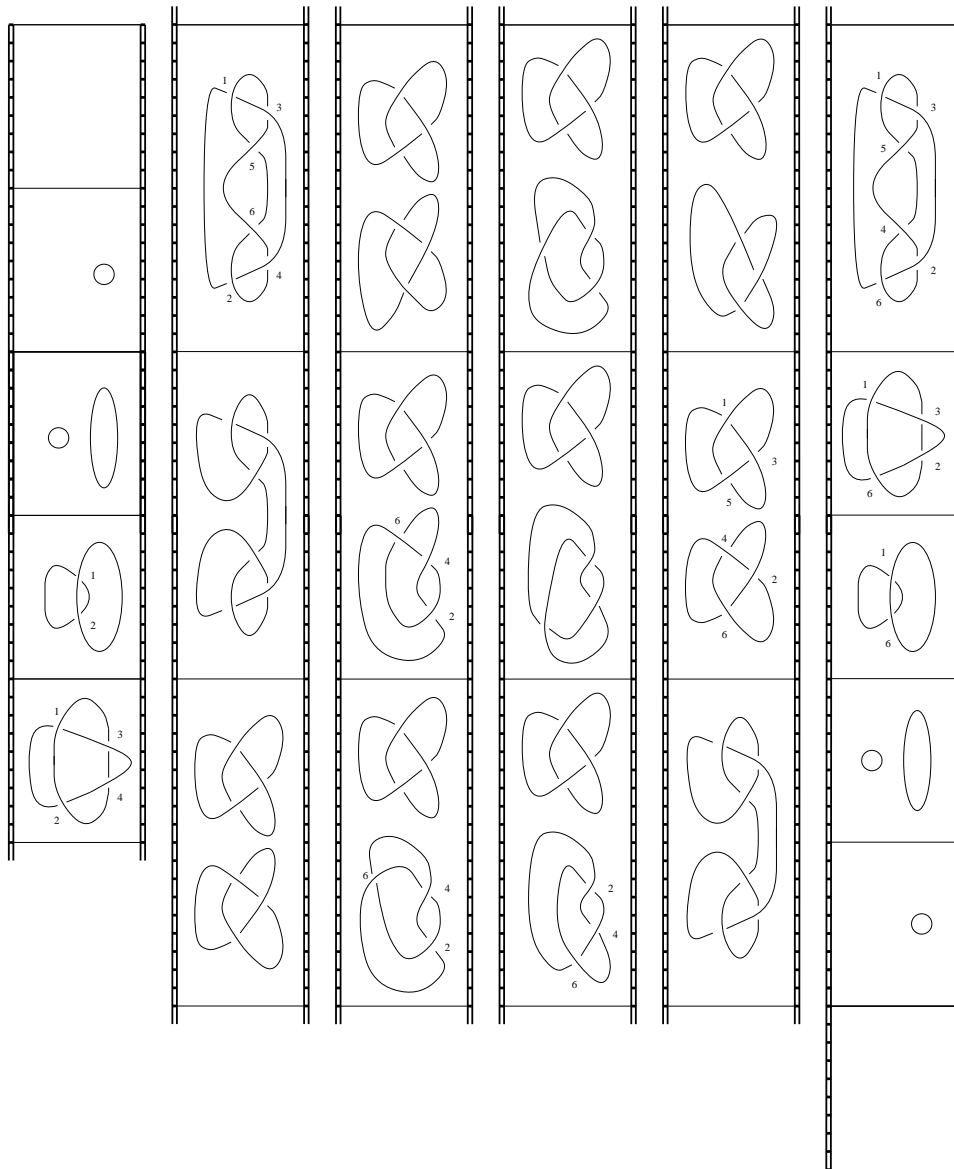


Figure 43: The movie of the example

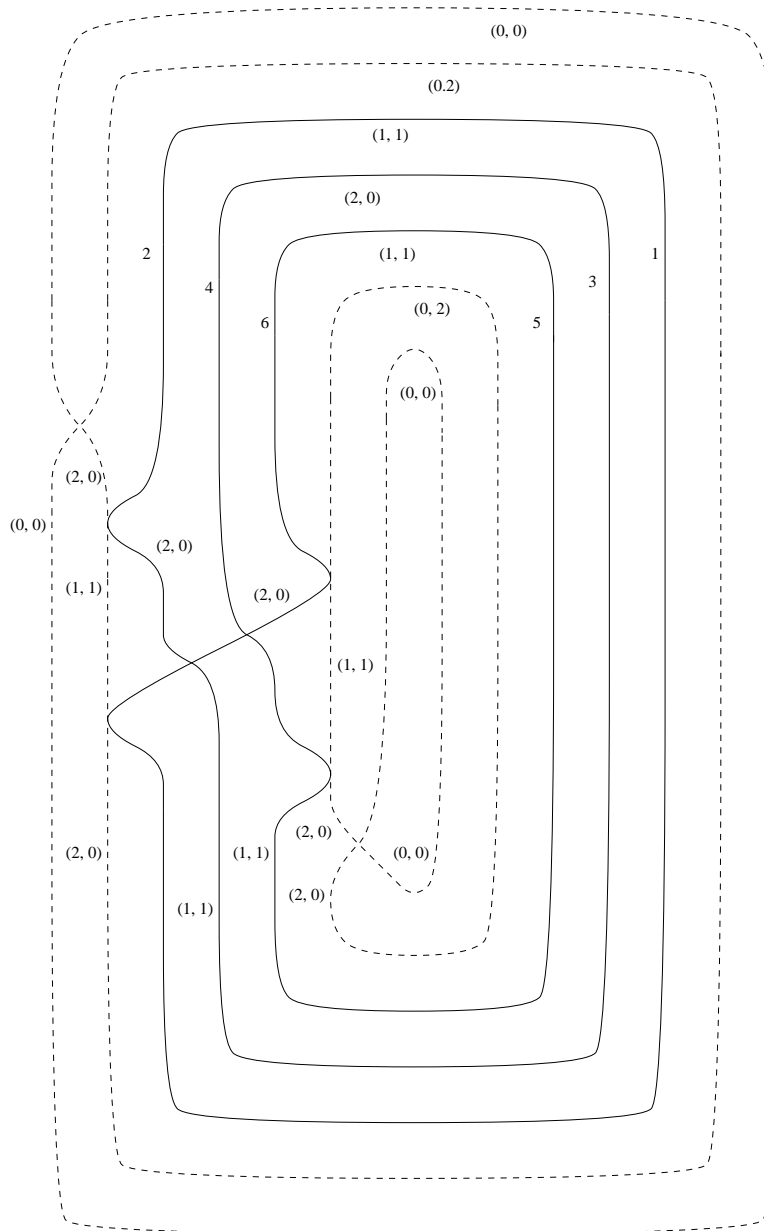


Figure 44: Its chart

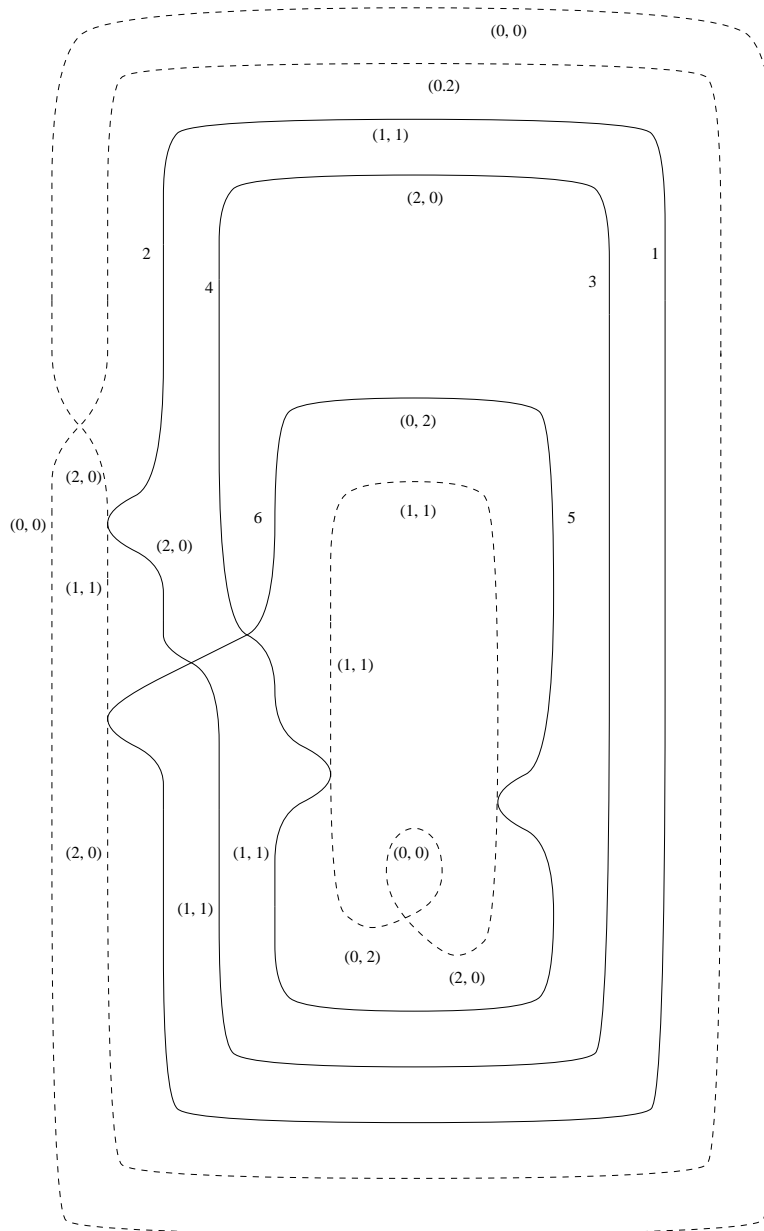


Figure 45: A modification

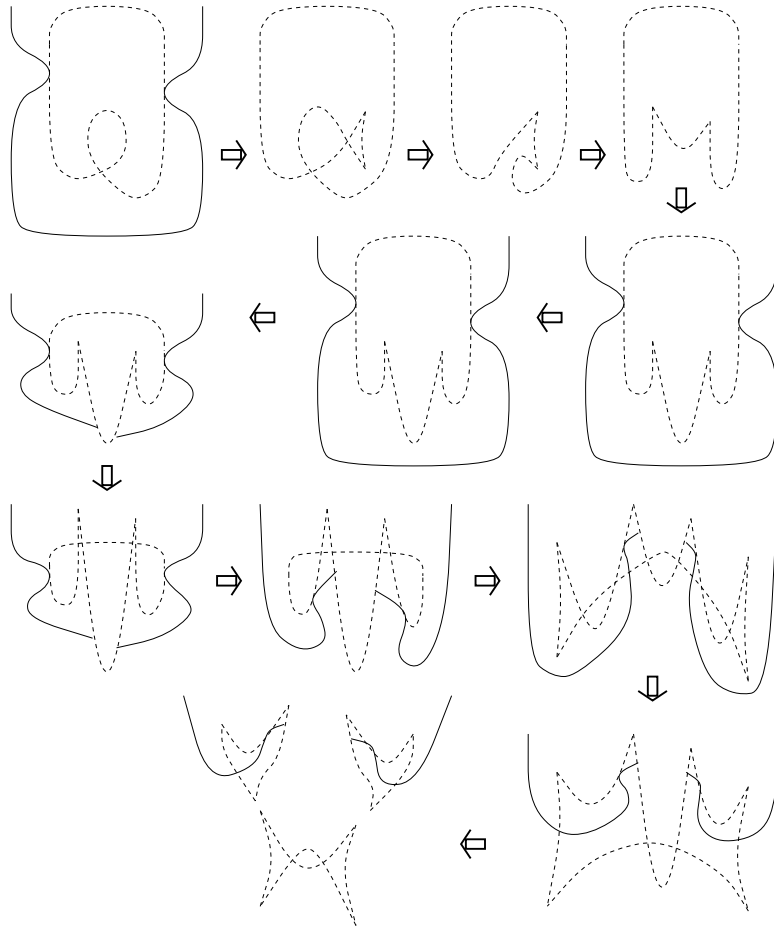


Figure 46: Chart Moves

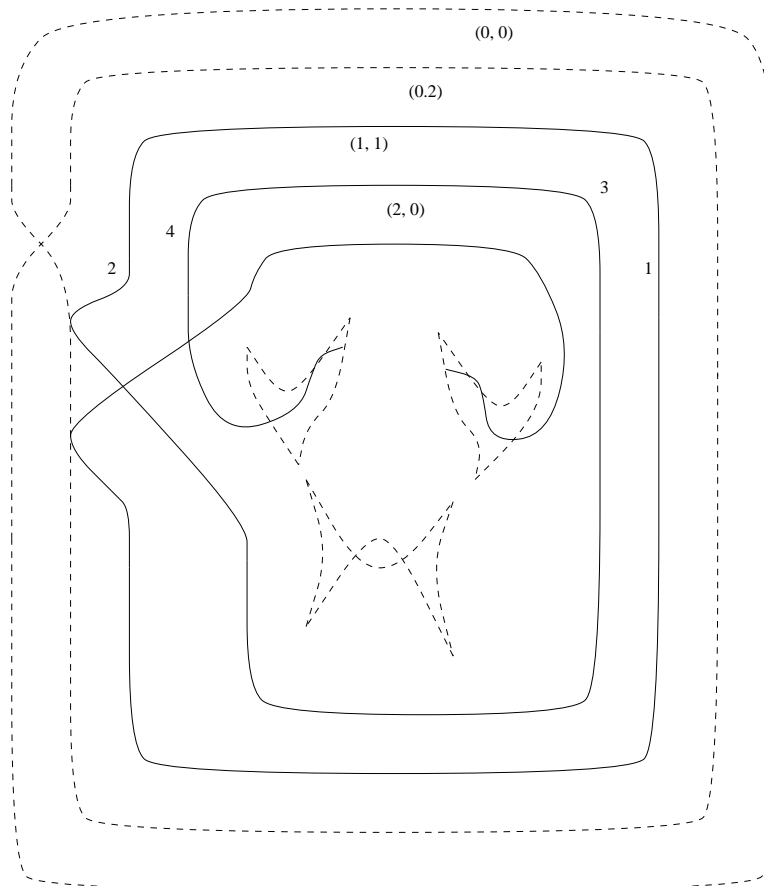


Figure 47: New chart

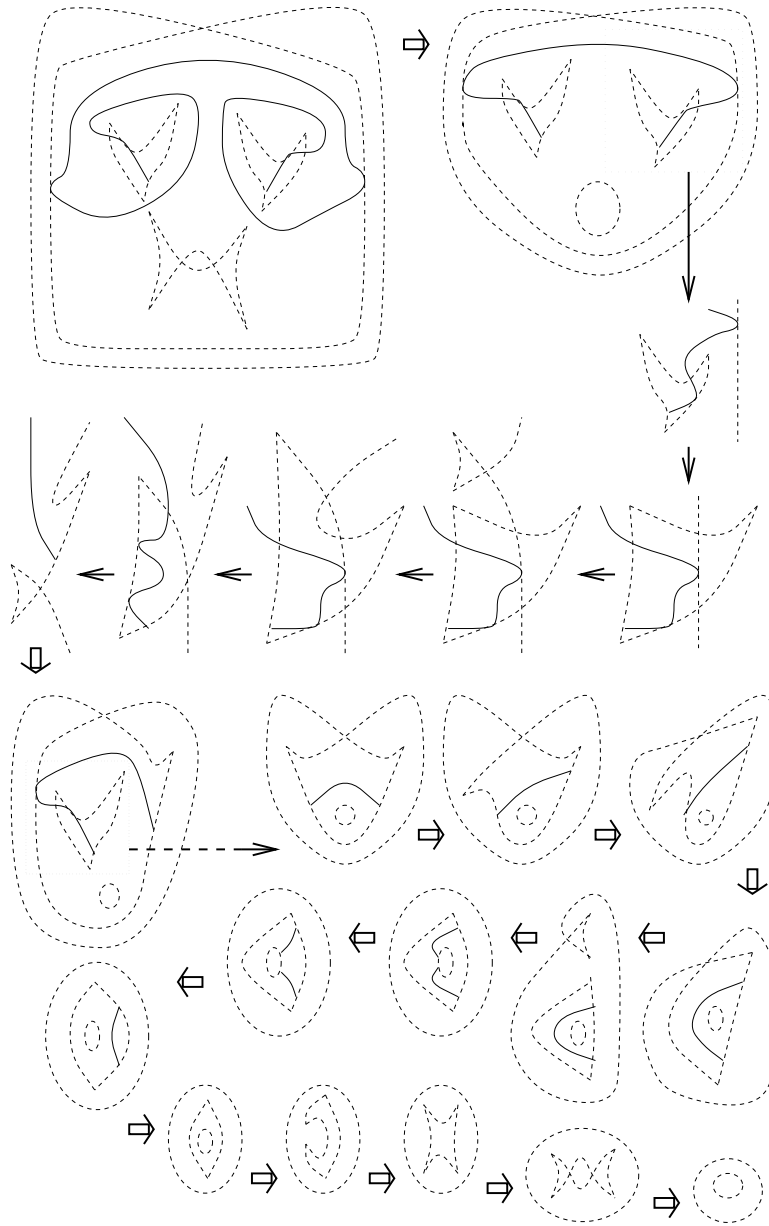


Figure 48: More chart moves

study and we hope that our diagrammatic results will provide the fundamental machinery for the study.

References

- [1] Abe, Eiichi, “Hopf Algebras,” Cambridge University Press, 1977.
- [2] Baez, John, and Dolan, James, *Higher-dimensional Algebra and Topological Quantum Field Theories*, J. Math. Phys. 36 (1995) 6073-6105.
- [3] Baez, John and Neuchl, M., *Higher-Dimensional Algebra I : Braided Monoidal 2-Categories*, to appear in Adv. Math.
- [4] Biedenharn, L. C., and Louck, J. D., “The Racah-Wigner Algebra in Quantum Theory,” Encyclopedia of Mathematics, Addison-Wesley (1981).
- [5] Boyle, Jeffrey *The turned torus knot in S^4* , Journal of Knot Theory and its Ramifications 2 (1993), no 3, 239–249.
- [6] Carter, J. Scott, “How Surfaces Intersect in Space: an Introduction to Topology,” World Scientific Publishing, 2nd edition (Singapore 1995).
- [7] Carter, J. Scott and Saito, Masahico, *Szygies among Elementary String Interactions in Dimension $2+1$* , Letters in Mathematical Physics 23 (1991), 287-300.
- [8] Carter, J. Scott, and Saito, Masahico, *Reidemeister Moves for Surface Isotopies and Their Interpretation as Moves to Movies*, J. of Knot Theory and its Ram., vol. 2, no. 3, (1993), 251-284.
- [9] Carter, J. Scott, and Saito, Masahico, *Braids and Movies*, to appear Journal Knot Theory and its Ramifications.
- [10] Carter, J. Scott, and Saito, Masahico, *Knotted Surfaces, Braid Movies and Beyond*, in Baez, J., “Knots and Quantum Gravity,” Oxford Science Publishing (Oxford 1994), 191-229.
- [11] Carter, J. Scott, and Saito, Masahico, *Knot Diagrams and Braid Theories in Dimension 4*, The Proceedings of the 3rd International Conference on Real and Complex Singularities, ed. Marar.

- [12] Carter, J. Scott, Flath, Daniel E., and Saito, Masahico “The Classical and Quantum $6j$ -symbols,” Princeton University Press Lecture Notes in Math Series (1995).
- [13] Carter, J.S., Rieger, J.H., and Saito, M., *A combinatorial description of knotted surfaces and their isotopies*, to appear Adv. in Math.
- [14] Chung, S., Fukuma, M., and Shapere, A., *Structure of topological lattice field theories in three dimensions*, Preprint, hep-th 9305080.
- [15] Crane, L., and Frenkel, I., *Four-dimensional topological quantum field theory, Hopf categories, and the canonical bases*, Topology and physics. J. Math. Phys. 35 (1994), no. 10, 5136–5154.
- [16] Crane, L., Kauffman, L. H., and Yetter, D., *Evaluating the Crane-Yetter Invariant*, in Kauffman and Baddhio, “Quantum Topology,” World Scientific Publishing (1992), 131-138.
- [17] Dijkgraaf, R., and Witten, E., *Topological gauge theories and group cohomology*, Comm. Math. Phys. 129 (1990), 393-429.
- [18] Drinfel’d, *Quantum Groups*, Proc ICM-86 (Berkeley) vol. 1 Amer. Math. Soc. (1987), 798-820.
- [19] Fischer, John *2-categories and 2-knots*, Duke Journal of Mathematics 75, No 2, (August 1994).
- [20] Freyd, P. J. and Yetter, D. N., *Braided Compact Closed Categories with Applications to Low Dimensional Topology*, Advances in Math. 77 (1989), 156-182.
- [21] M. Fukuma, S. Hosono, and H. Kawai, *Lattice topological field theory in two dimensions*, Cornell preprint, hep-th/9212154.
- [22] Gelfand, I.M., Kapranov, M.M., and Zelevinsky, A. V., *Newton polytopes of principal A -discriminants*, Soviet Math. Doklady 40 (1990), 278-281.
- [23] Gelfand, I. M., Kapranov, M. M., and Zelevinsky, A. V., “Discriminants, resultants, and multidimensional determinants”, Birkhauser Boston, Inc., Boston, MA, 1994.
- [24] Giller, Cole, *Towards a Classical Knot Theory for Surfaces in \mathbf{R}^4* , Illinois Journal of Mathematics 26, No. 4, (Winter 1982), 591-631.

- [25] Goodman, F. M. and Wentzl, H., *The Temperley-Lieb Algebra at Roots of Unity*, Pacific Journal of Math. Vol 161, No.2 (1993), 307-334.
- [26] Goryunov, V. V., *Monodromy of the Image of a Mapping*, Functional Analysis and Applications 25 (1991), 174-180.
- [27] Jones, V. F. R., *A Polynomial Invariant for Knots and Links via von Neumann Algebras*, Bull. AMS 12 (1985), 103-111 .
- [28] Kamada, Seiichi, *Surfaces in R^4 of braid index three are ribbon*, Journal of Knot Theory and its Ramifications 1 (1992), 137-160.
- [29] Kamada, Seiichi, *2-dimensional braids and chart descriptions*, "Topics in Knot Theory", Proceedings of the NATO Advanced Study Institute on Topics in Knot Theory, Turkey, (1992), 277-287.
- [30] Kauffman, L. H., "Knots and Physics", World Sci. , 1991.
- [31] Kauffman, L. H., and S. L. Lins, "Temperley-Lieb Recoupling Theory and Invariants of 3-manifolds," Princeton U. Press, 1994.
- [32] Kauffman, L. H., *Spin networks, Topology and Discrete Physics* reprinted in the second edition of "Knots and Physics," World Science Publishing (1993)
- [33] Kapranov, M. and Voedvodsky, V., *Braided Monoidal 2-Categories and Manin-Schectman Higher Order Braid Groups*, J. Pure and Applied Algebra 92 (1994), 241-267.
- [34] Kharlamov, V.M., and Turaev, V.G. *On the 2-category of 2-knots*, Preprint March 1994.
- [35] Kirillov, A. N. and Reshetikhin, N. Yu, *Representations of the Algebra $U_q(sl(2))$, q -Orthogonal Polynomials and Invariants of Links*. Reprinted in Kohno "New Developments in the Theory of Knots," World Scientific Publishing (1989).
- [36] Kuperberg, G., *Involutory Hopf algebras and 3-manifold invariants*, Internat. J. Math. 2 (1991), no. 1, 41-66.
- [37] Livingston, C., *Stably irreducible surfaces in S^4* . Pacific Journal of Math 116 (1985), no 1, 77-84.
- [38] Mancini, S. and Ruas, M.A.S., *Bifurcations of generic 1-parameter families of functions on foliated manifolds*, Math. Scand. 72 (1993), 5-15.

- [39] Markl, M., Stasheff, J.D., *Deformation theory via deviations*, The Proceedings of the Winter School Geometry and Topology (1992). Rend. Circ. Mat. Palermo (2) Suppl. No. 32 (1993), 97–124.
- [40] Mond, D. *On the Classification of Germs of Maps from \mathbf{R}^2 to \mathbf{R}^3* , Proc LMS 50 (1985), 333-369.
- [41] Mond, D. *Singularities of Mappings from Surfaces to 3-Space*, Proceedings of International Summer School on Singularities, ICTP, Trieste (1991).
- [42] Pachner, U., *PL homeomorphic manifolds are equivalent by elementary shelling*, Europ. J. Combinatorics Vol. 12 (1991), 129-145.
- [43] Penrose, R., *Applications of Negative Dimensional Tensors*, in Welsh, “Combinatorial Mathematics and its Applications,” Academic Press (1971).
- [44] Reiner, V., and Ziegler, G.M., *Coxeter-associahedra*, Mathematika, 41 (1994), 364-393.
- [45] Reidemeister, K., “Knotentheorie,” Chelsea Publishing CO., NY (1948). Copyright 1932, Julius Springer, Berlin.
- [46] Reshetikhin, N.Y., and Turaev, V., *Invariants of three manifolds via link polynomials and quantum groups*, Invent. math. 103 (1991), 547-597.
- [47] Rieger, J. H., *On the complexity and computation of view graphs of piecewise smooth algebraic surfaces*, Phil. Trans. R. Soc. London Ser. A (in press).
- [48] Roseman, Dennis, *Reidemeister-Type Moves for Surfaces in Four Dimensional Space*, Preprint.
- [49] Roseman, Dennis, *Twisting and Turning in Four Dimensions*, A video made at the Geometry Center (1993).
- [50] Stasheff, J.D., *Homotopy associativity of H-spaces*, Trans. A.M.S., 108 (1963), 275-292.
- [51] Turaev, V. *Operator Invariants of tangles, and R-matricies*, Math USSR Izvestia, 35 (1990), 411-444.
- [52] Turaev, V., “Quantum Invariants of Knots and 3-Manifolds,” de Gruyter Publishing, Berlin (1995).

- [53] Turaev, V., and Viro, O. Ya., *State Sum Invariants of 3-manifolds and Quantum 6j-symbols*, Topology 31 (1992), 865-902.
- [54] Wall, C.T.C., *Finite determinacy of smooth map-germs*, Bull. London Math. Soc. (1981) 13, 481-539.
- [55] West, J. M., "The differential geometry of the crosscap," Ph.D. thesis, Univ. of Liverpool, England, 1995.
- [56] Yoshikawa, K., *An Enumeration of Surfaces in Four Space* , Osaka J. Math., 31 (1994), 497-522.